

**Greenland Analogue Project – Hydraulic properties of deformation zones and fracture domains at Forsmark, Laxemar and Olkiluoto for usage together with Geomodel version 1**

Sven Follin, SF GeoLogic AB

Martin Stigsson, Svensk Kärnbränslehantering AB

Ingvar Rhén, Sweco Environment AB

Jon Engström, Geologian tutkimuskeskus

Knut Erik Klint, De Nationale Geologiske Undersøgelser for Danmark og Grønland

May 2011

**Svensk Kärnbränslehantering AB**

Swedish Nuclear Fuel  
and Waste Management Co

Box 250, SE-101 24 Stockholm  
Phone +46 8 459 84 00



# **Greenland Analogue Project – Hydraulic properties of deformation zones and fracture domains at Forsmark, Laxemar and Olkiluoto for usage together with Geomodel version 1**

Sven Follin, SF GeoLogic AB

Martin Stigsson, Svensk Kärnbränslehantering AB

Ingvar Rhén, Sweco Environment AB

Jon Engström, Geologian tutkimuskeskus

Knut Erik Klint, De Nationale Geologiske Undersøgelser  
for Danmark og Grønland

May 2011

Data in SKB's database can be changed for different reasons. Minor changes in SKB's database will not necessarily result in a revised report. Data revisions may also be presented as supplements, available at [www.skb.se](http://www.skb.se).

A pdf version of this document can be downloaded from [www.skb.se](http://www.skb.se).

## Abstract

The database of the GAP site is under development. In order to meet the data needs of the different modelling teams working with groundwater flow modelling it has been decided to compile trial data sets comprising structural-hydraulic properties suitable for flow modelling on different scales. The properties provided in this report are based on data and groundwater flow modelling studies conducted for three sites located in the Fennoscandian Shield, two of which are studied by SKB, Forsmark and Laxemar, and one by Posiva, Olkiluoto. The provided hydraulic properties provided here are simplified to facilitate a readily usage together with the GAP Geomodel version 1.

## Sammanfattning

Arbetet med att ta fram en databas för GAP pågår. I syfte att tillgodose databehovet hos de pågående flödesmodelleringarna beslutades att ta fram övningsdata avseende strukturella och hydrauliska egenskaper i olika modellskalor. De egenskaper som föreslås i denna rapport är hämtade från grundvattenmodelleringar som utförts på tre olika platser inom den Fennskandiska Skölden. Två av platserna, Forsmark och Laxemar, har undersökts av SKB medan den resterande platsen, Olkiluoto, har undersökts av Posiva. Sammanfattningvis har de hydrauliska egenskaperna som presenteras i denna rapport förenklats i syfte underlätta deras användning tillsammans med GAP Geomodell version 1.

## Tiivistelmä

GAP tutkimusalueelta on valmisteilla tietokanta pohjaveden virtausmallinnusryhmien käyttöön. Tämä alustava tietokanta sisältää tietoa kallioperän rakenteellista ja hydraulisista ominaisuuksista ja sitä voidaan käyttää hyväksi eri mittakaavaisissa mallinnustarkasteluissa. Tässä raportissa annettu ominaisuustieto perustuu kolmesta Fennoskandian kilvellä sijaitsevasta kohteesta kerättyyn aineistoon ja niissä tehtyyn virtausmallinnukseen. Kaksi näistä kohteista on SKB:n tutkimia, Forsmark ja Laxemar, ja kolmas on Posivan tutkima Olkiluoto. Raportissa annettu hydraulinen ominaisuustieto on yksinkertaistettua ja yleistettyä, jotta sen käyttö yhdessä GAP Geomalli versio 1 kanssa olisi mahdollisimman helppoa.

# Contents

<b>1</b>	<b>Introduction</b>	7
1.1	Background	7
1.2	Systems approach	8
1.3	Scope and objectives	8
1.4	Relation between flow concepts	8
1.5	Outline of report	9
<b>2</b>	<b>Summary of the GAP Geomodel version 1</b>	11
2.1	Location	11
2.2	Description	12
2.3	Structural and geometrical properties	12
2.4	Stresses	15
2.5	3D visualisation	16
2.6	Groundwater flow modelling domains	17
<b>3</b>	<b>Geological settings of Forsmark, Laxemar and Olkiluoto</b>	19
3.1	Forsmark	19
3.2	Laxemar	21
3.3	Olkiluoto	24
<b>4</b>	<b>Hydrogeological properties – Forsmark</b>	27
4.1	Main hydraulic characteristics	27
4.2	Deformation zones	27
4.2.1	Transmissivity	27
4.2.2	Stresses	28
4.3	Rock mass volumes between deformation zones	29
4.3.1	DFN properties	29
4.3.2	ECPM properties	29
4.3.3	CPM and SC properties	29
<b>5</b>	<b>Hydrogeological properties – Laxemar</b>	31
5.1	Main hydraulic characteristics	31
5.2	Deformation zones	31
5.2.1	Transmissivity	31
5.2.2	Stresses	31
5.3	Rock mass volumes between deformation zones	32
5.3.1	DFN properties	32
5.3.2	ECPM properties	32
5.3.3	CPM and SC properties	32
<b>6</b>	<b>Hydrogeological properties – Olkiluoto</b>	35
6.1	Main hydraulic characteristics	35
6.2	Hydro-zones	35
6.2.1	Transmissivity based on injections tests and pumping tests	35
6.2.2	Transmissivity based on difference flow logging	35
6.2.3	Stresses	36
6.3	Rock mass volumes between deformation zones	36
6.3.1	DFN properties	36
6.3.2	ECPM properties	36
6.3.3	CPM and SC properties	37
<b>7</b>	<b>Storage and transport properties</b>	39
7.1	Specific storage and storativity	39
7.2	Kinematic porosity	39
7.3	Transport aperture	42
7.4	Travel time	43

<b>8</b>	<b>Recommendations for flow modellers</b>	45
8.1	General	45
8.2	Usage of HCD properties	45
8.3	Usage of HRD properties	46
8.4	HCD and HRD properties below –1,000 m elevation	46
8.5	On the modelling of deformation zones outside the area covered by the GAP Geomodel version 1	47
<b>9</b>	<b>References</b>	49
<b>Appendix 1</b>	<b>3D structural-hydraulic model</b>	51

# 1 Introduction

## 1.1 Background

The database of the GAP site is under development. At the 2nd annual GAP modelling workshop in Toronto, November 2011, an update of the geological map and deformation zone model of the field area around Kangerlussuaq was requested by the groundwater flow modellers. This was mainly due to the very simple and stochastic nature of the previous model, which was based on superficial interpretation of site scale lineaments and the mapping data collected from small key areas in 2008. Second, in order to meet the data needs of the different modelling teams working with groundwater flow modelling it was decided to compile trial data sets comprising structural-hydraulic properties suitable for flow modelling on different scales. The properties provided in this report are based on data and groundwater flow modelling studies conducted for three sites located in the Fennoscandian Shield, two of which are studied by SKB, Forsmark and Laxemar, and one by Posiva, Olkiluoto, see Figure 1-1.

It is noted that few of the hydraulic investigations at Forsmark, Laxemar and Olkiluoto are deeper than 1 km. Hence there are great uncertainties involved when hydraulic data from these three sites are adapted to the 5 km deep deformation zone model at the GAP site. In particular, this alert concerns the usage of data from Olkiluoto as there is no depth trend specified at this site. The provided hydraulic properties are simplified to facilitate a readily usage together with the GAP Geomodel version 1 /Engström et al. 2011/. The hydraulic properties reported here are based on the information provided by /Ahokas et al. 2007, Follin et al. 2007, Follin 2008, Hartley et al. 2009, Hjerne et al. 2010, Rhén et al. 2008, Rhén and Hartley 2009, Vaittinen et al. 2009/.



*Figure 1-1. Locations of Olkiluoto, Forsmark and Laxemar and the Fennoscandian Shield.*

## 1.2 Systems approach

Figure 1-2 illustrates a division of the groundwater system into three hydraulic domains, HCD, HRD and HSD, where:

- HCD (Hydraulic Conductor Domain) represents deformation zones (DZ),
- HRD (Hydraulic Rock mass Domain) represents the less fractured rock mass volumes (fracture domains) between the deformation zones, and
- HSD (Hydraulic Soil Domain) represents the regolith (Quaternary deposits).

## 1.3 Scope and objectives

The main objective of this report is to provide hydraulic properties of deformation zones, HCD, and rock mass volumes between zones, HRD, regardless of the flow concept used. The flow concepts in mind are:

- Stochastic groundwater flow modelling using the discrete fracture network (DFN) approach and/or the equivalent continuous porous medium (ECPM) approach.
- Stochastic groundwater flow modelling using the stochastic continuum (SC) approach.
- Continuum groundwater flow modelling using the homogeneous continuous porous medium (CPM) approach.

## 1.4 Relation between flow concepts

Groundwater flow in crystalline rock occurs in discrete fracture networks (DFN). The properties of a DFN model are generally site specific and, notably, within a given site, several DFN models are generally used. A common approach is to divide each HRD into one or several so-called fracture domains. Within each fracture domain, the parameter values of the following structural-hydraulic property models are fixed:

- Position
- Orientation
- Size
- Intensity
- Transmissivity
- Transport aperture.

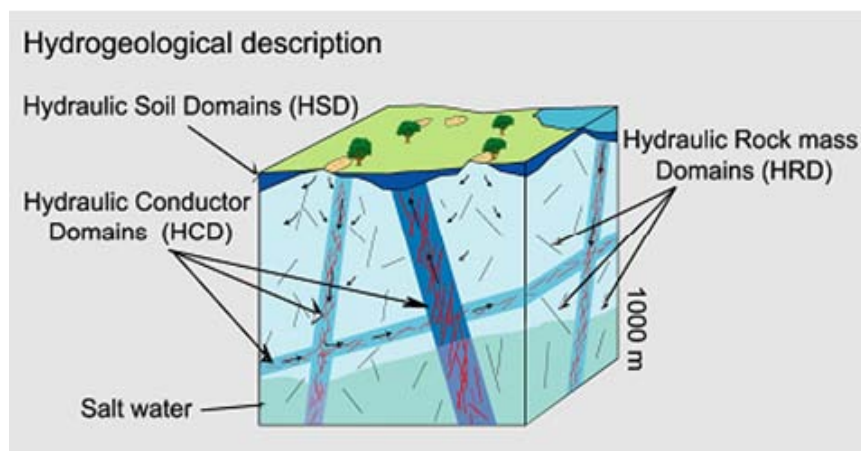


**Figure 1-2.** Cartoon showing the division of the crystalline bedrock and the regolith (Quaternary deposits) into three hydraulic domains, HCD, HRD and HSD.

By definition, DFN modelling invokes Monte Carlo simulations (multiple realisations) as the property models are described statistically. Uncertainties associated with the choice of property models are generally taken care of by means of a sensitivity analysis. That is, besides multiple realisations for a given set-up of property models, model variants are used.

Equivalent continuous porous medium (ECPM) properties are obtained from fracture network (DZ and DFN) realisations by means of up-scaling. Since each ECPM model studied is based on a particular underlying stochastic DFN realisation, the ECPM models are also stochastic. The method used for up-scaling varies between modelling tools. However, typical for the ECPM concept is that the heterogeneity and anisotropy of an ECPM realisation depend on:

- the characteristics of the underpinning fracture network realisation, and
- the chosen support scale (resolution) of the ECPM computational grid.

In contrast to the ECPM concept, stochastic continuum (SC) properties are not commonly obtained from DFN realisations by means of up-scaling, but generally based on *in-situ* hydraulic conductivity data  $K$  [ $LT^{-1}$ ; m/s] measured between packers in boreholes. Generally, hydraulic conductivity data from packer tests can be matched to a lognormal distribution,  $Y=\log(K)$ , hence the statistical moments of interest are the arithmetic mean, the standard deviation and the covariance of  $Y$ . Notably, the statistical moments may be heterogeneous, e.g. possess a depth dependence.

The stochastic continuum concept is essentially an elaboration of the classic continuous porous medium (CPM) concept. A model that is based on the latter concept invokes the notion of a representative elementary volume (REV). In conclusion, the CPM concept implies homogeneity, where the homogenous value is simply the geometric mean of *in-situ* hydraulic conductivity data  $K$ . Depth dependence is allowed, however.

## 1.5 Outline of report

The outline of the report is as follows:

- Chapter 2 presents a summary of Geomodel version 1.
- Chapter 3 briefly presents the geology of Forsmark, Laxemar and Olkiluoto.
- Chapter 4 presents the suggested hydraulic properties for Forsmark.
- Chapter 5 presents the suggested hydraulic properties for Laxemar.
- Chapter 6 presents the suggested hydraulic properties for Olkiluoto.
- Chapter 7 presents some recommendations for flow modellers.



## 2 Summary of the GAP Geomodel version 1

### 2.1 Location

Geomodel version 1 utilises all available information (geological, topographical and geophysical) in order to improve the accuracy of the model, especially in the area covered by the ice sheet. The modelling area was divided into two scales; a regional scale area and a site scale area as shown in Figure 2-1. The GAP site scale refers to the area where surface mapping has been performed, and where DH-GAP01 and DH-GAP03 were drilled during 2009.

The coordinates of the modelling area (regional area, lilac rectangle in Figure 2-1 are:

NW corner: 214504; 7508404  
NE corner: 319746; 7495482  
SW corner: 206444; 7442218  
SE corner: 311563; 7429378

These coordinates are in the Projected Coordinate System NAD 1983 Complex UTM Zone 23N, for which the GEUS geological map applies. However, the GAP project database is in the Projected Coordinate System WGS 1984 Complex UTM Zone 22N. The coordinates in this system of the modeling area are:

NW corner: 469885; 7493368  
NE corner: 576217; 7490673  
SW corner: 468187; 7426678  
SE corner: 574508; 7423937

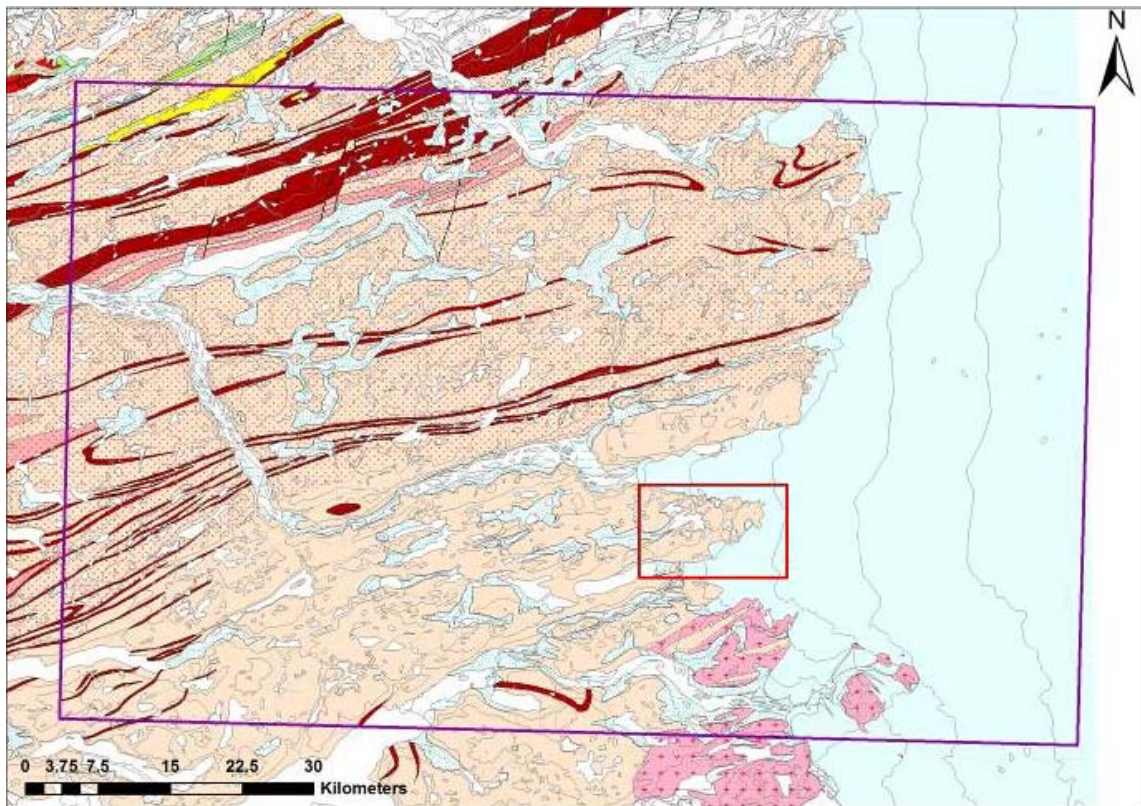


**Figure 2-1.** Map showing the regional modelling area of Geomodel version 1 in lilac and the GAP site scale area in red. Geomodel version 1 covers an area of approximately 70 km by 110 km. Geology is adapted from GEUS Geological map /Escher 1971/.

The GAP site area (the smaller red rectangle in Figure 2-1) has the following coordinates:

NW corner: 528881; 7451274  
NE corner: 544208; 7451274  
SW corner: 528881; 7441489  
SE corner: 544208; 7441489

## 2.2 Description

The work on Geomodel version1 started in January 2011, although some work on the site scale model and ideas for the regional model was already initiated in 2010. This work included processing of mapping data that the GAP project collected during 2008–2010 and the analysis of fracture data from the pilot holes drilled in 2009. First, a regional lineament map was produced by integrating geological information and topographical indications. Second, an independent geophysical lineament interpretation was done using aeromagnetic data provided by GEUS. Third, the two lineament interpretations were integrated into a 2D model with a total of 158 deformation zones/faults, see Figure 2-2 and Figure 2-3; 53 were interpreted from the geological/topographical data solely, 51 were interpreted from the geophysical data solely, and 54 were common to both interpretations.

The integrated modelling revealed four different sets of potential deformation zones and faults. These were designated individual colour codes to easily distinguish them from each other. The Type 1 set (Lilac) trends ENE-WSW. It crosscuts the area. The Type 2 set (Green) trends NW-SE and the Type 3 set (Blue) trends NE-SW. The Type 2 and the Type 3 sets are both shorter than the Type 1 set and might be a conjugate system with each other. The Type 4 set (Black) trends NNE-SSW and crosscuts all other types, hence it is the youngest of the four sets. The Type 4 set is possibly related to the same event as the faults on the western coast of Greenland which formed during the continental break-up when Greenland started to drift apart from Canada.

The geological/topographical interpretation includes more of Type 4, whereas the geophysical interpretation contains more of Type 1. Eighteen of 158 deformation zones/faults occur within the site scale area shown in Figure 2-1 and most of them are supported by field observations.

## 2.3 Structural and geometrical properties

As stated above, the 158 lineaments interpreted in the integrated modelling are interpreted to belong to four different types of steeply dipping deformation zones/faults<sup>1</sup>. From the site scale data it is also evident that a fifth, sub-horizontal set of deformation exists. However, due to the spatially limited information, its character and occurrence on a regional scale is difficult to delineate.

The five different types of deformation zones/faults are classified as follows:

### **Type 1 (Lilac)**

Character: Larger scale deformation zones with both ductile and brittle deformations  
Count: 45  
Trend: ENE-WSW  
Dip: N, steep to moderate (approximately 75°)

### **Type 2 (Green)**

Character: Smaller scale deformation zones/faults of mainly brittle character  
Count: 24  
Trend: NW-SE  
Dip: NE (18) and SW (6), steep to moderate (approximately 75°)

---

<sup>1</sup> Deformations zones are larger and wider features, whereas faults are single features but larger than an ordinary fracture.

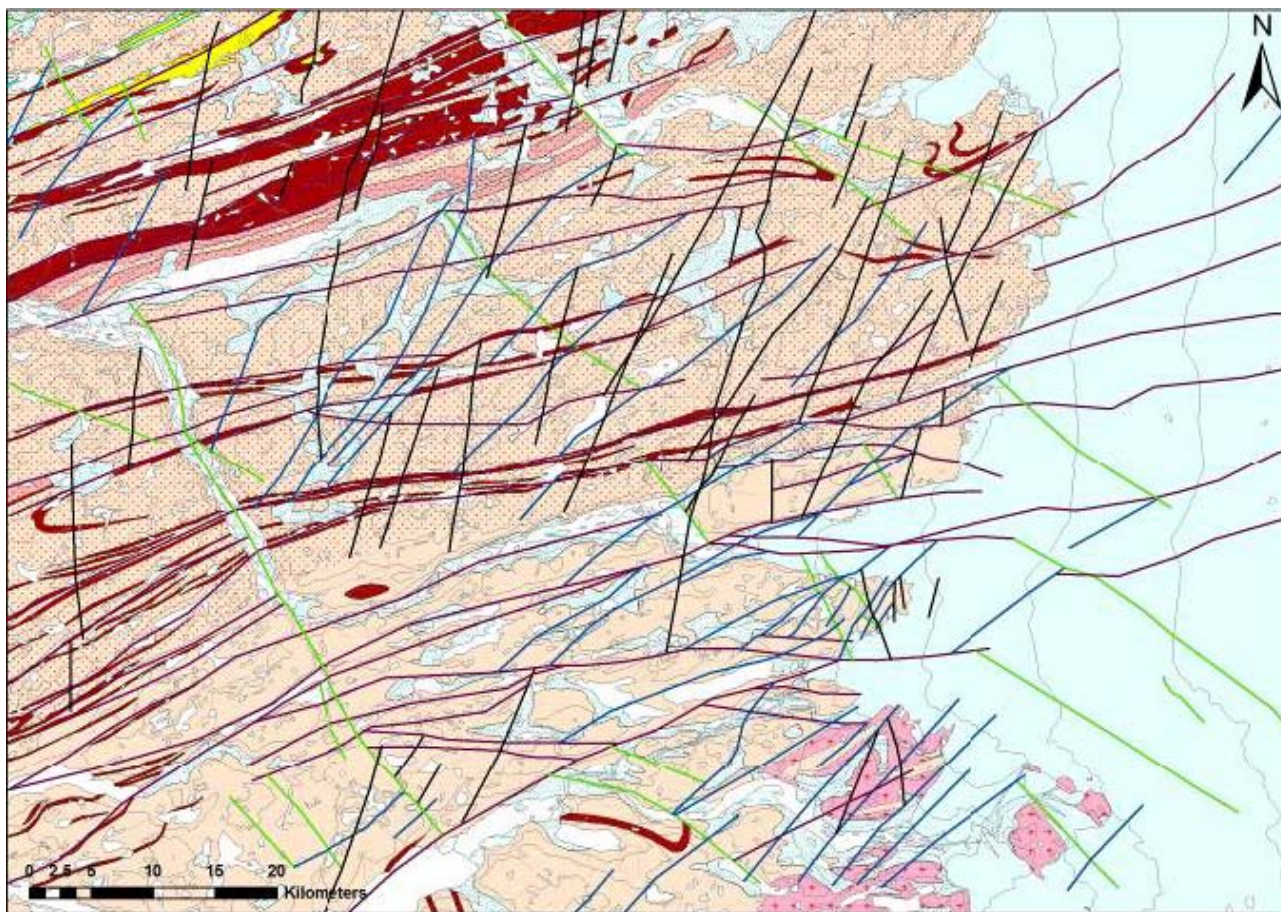


**Figure 2-2.** Map showing the final interpretation of Geomodel version 1 with the four different types of deformation zones and faults: Type 1=Lilac (oldest), Type 2=Green, Type 3=Blue and Type 4=Black (youngest). Geology is adapted from GEUS Geological map /Escher 1971/.

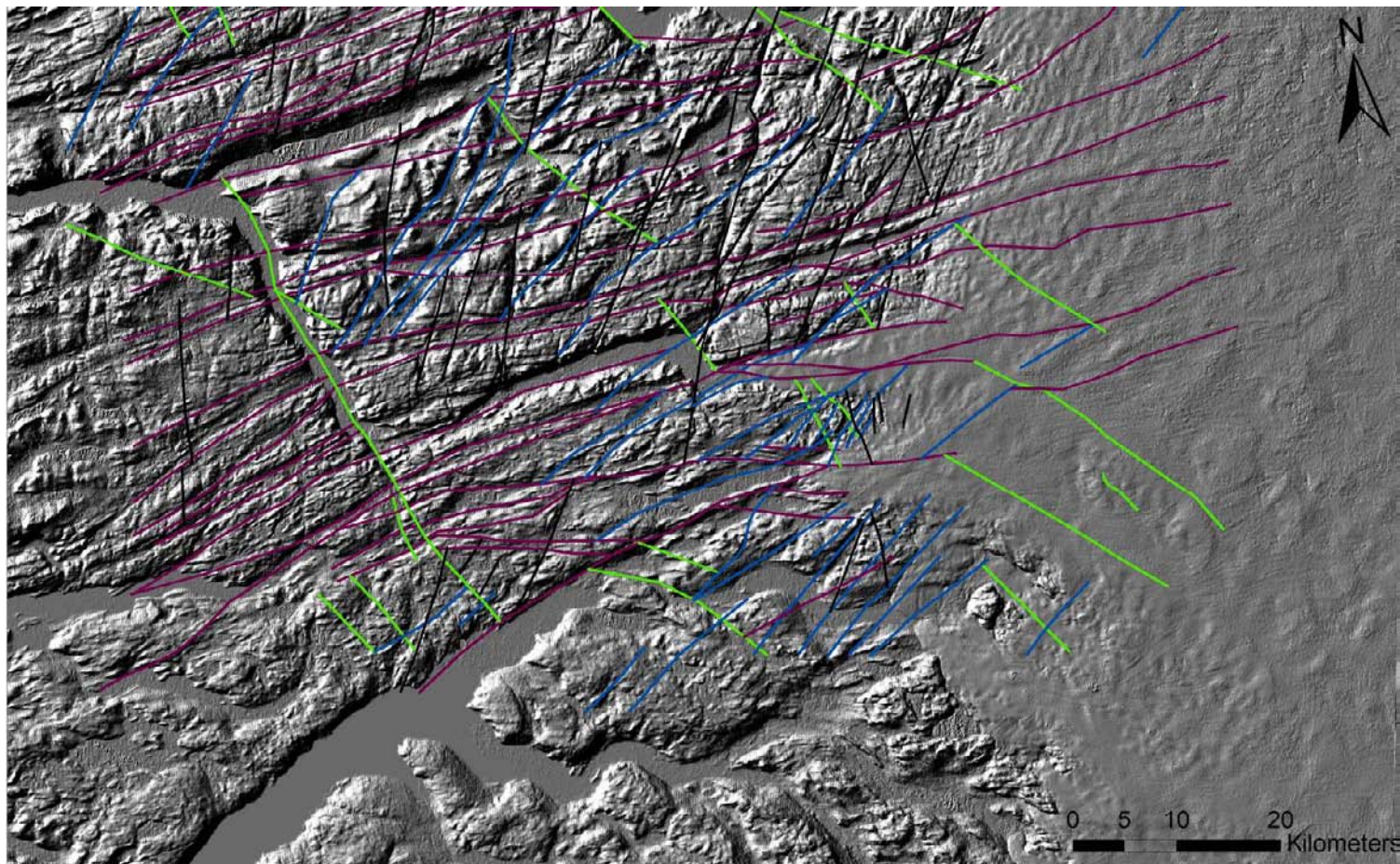


**Figure 2-3.** The same structural interpretation as shown in Figure 2-2 but superimposed on a topographical image. The fjords seen to the west of ice sheet margin might continue in under the ice sheet where they could be filled with debris such as glacial till and/or glaciofluvial sediments.

### **Type 3 (Blue)**

Character: Smaller scale deformation zones/faults of mainly brittle character  
Count: 43  
Trend: Mainly NE-SW  
Dip: SE (22) and NW (21), steep to moderate (approximately 70°)

### **Type 4 (Black)**

Character: Smaller scale faults of mainly brittle character  
Count: 46  
Trend: NNE-SSW  
Dip: E or W, essential vertical (approximately 85°)

### **Type 5 (Not modelled in Geomodel version 1)**

Character: Possibly site-scale deformation zones of mainly brittle character  
Count: N/A  
Trend: Possibly ENE-WSW.  
Dip: Possibly SE, gently dipping (approximately 15°)

## **2.4 Stresses**

The dominant stresses in West Greenland seems to be of extensional nature enhanced by the spreading of the continental lithosphere following the ongoing opening of Baffin Bay when Canada and Greenland started to drift apart approximately 100 million years ago.

At the western coast of Greenland the maximum horizontal stress trends NW-SE and the minimum horizontal stress trends NE-SW. The stress field at the GAP site can be different, however, because in this region the stress field from the old orogeny might still prevail. The presence of the Type 4 fault system, which is related to the opening of the Baffin Bay and Davis Strait, indicates prevailing stress conditions originating from this tectonic event. Furthermore, glacially induced stresses from the subsidence and rebound of the basement during numerous glaciations affecting the area over the last 2 million years, may likely dominate the prevailing stress conditions within the basement today, especially close to reactivated fault zones. Finally, the presence of deep permafrost may also affect the stress field (Figure 2-4).

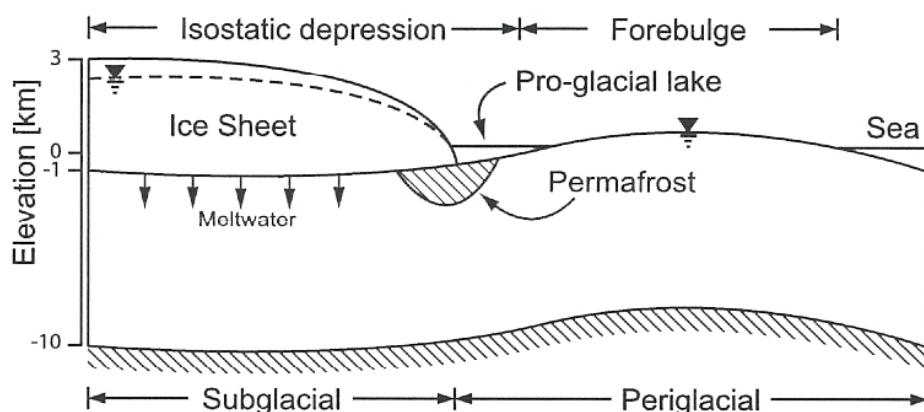


**Figure 2-4.** Cross section along an ice flow line showing hydraulic conditions and mechanical deformations in proximity of the ice sheet margin /Lemieux et al. 2008/.

## 2.5 3D visualisation

Figure 2-5 and Figure 2-6 show two images of Geomodel version 1. The horizontal axes in these images use the Bamber coordinate system /Bamber et al. 2001, Layberry and Bamber 2001/. More information about how the 3D modelling is made is provided in Appendix 1.

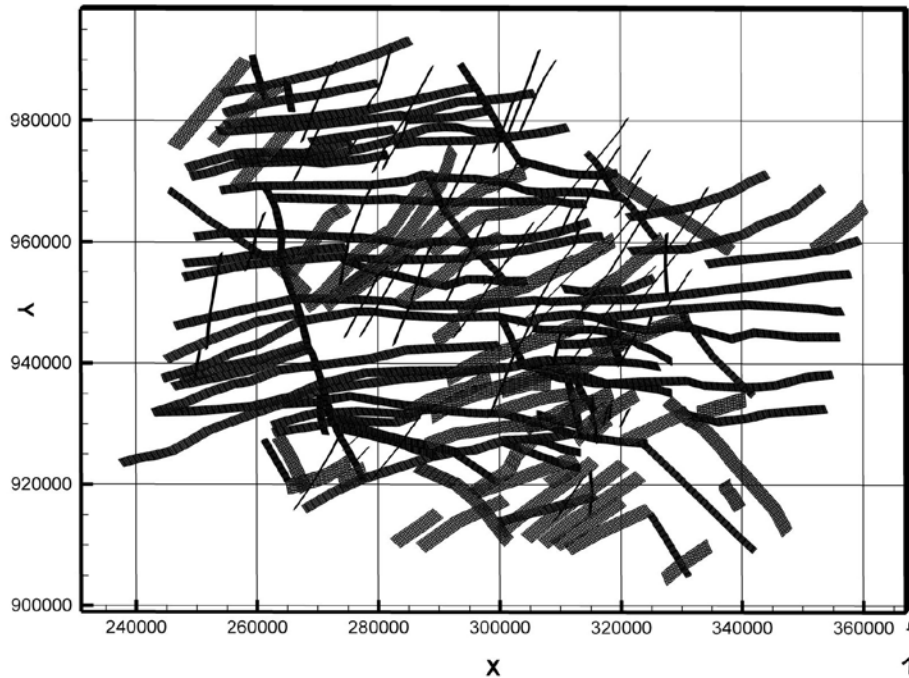


*Figure 2-5. Top view of Geomodel version 1 in Bamber coordinates.*

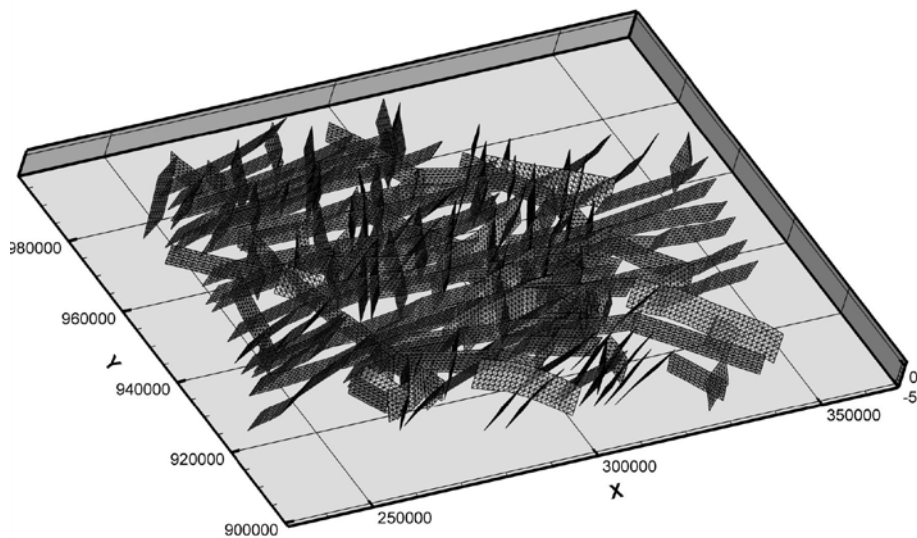


*Figure 2-6. Perspective view of Geomodel version 1 in Bamber coordinates. Each deformation zone/fault is extended to 5 km deep and triangulated vertically by means of 1 km large triangles.*

## 2.6 Groundwater flow modelling domains

Figure 2-7 shows horizontal views of the Geomodel version 1 vis-à-vis the tentative locations and sizes of three model domains that might be used for groundwater flow modelling with the GAP. The three model domains are coloured blue, red and yellow (1 smaller and 1 larger). A lilac colour is used where the blue and red model domains coincide.

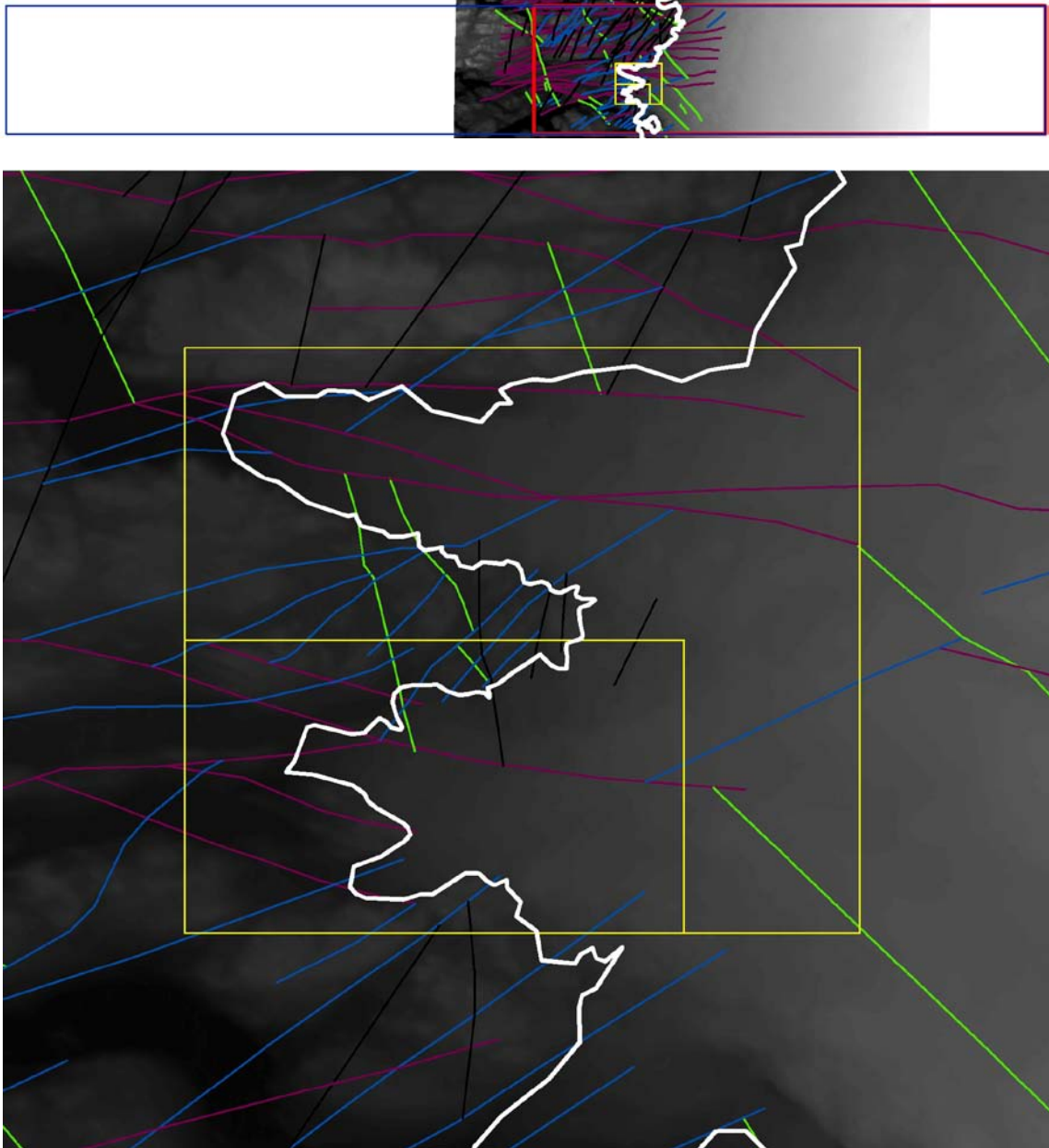


**Figure 2-7.** Horizontal views of Geomodel version 1 vis-à-vis the tentative locations and sizes of three model domains that might be used for groundwater flow modelling with the GAP. The three model domains are coloured blue, red and yellow (1 smaller and 1 larger). A lilac colour is used where the blue and red model domains coincide. The white line in each image indicates the location of the ice sheet margin.

### 3 Geological settings of Forsmark, Laxemar and Olkiluoto

The crystalline bedrock at Forsmark, Laxemar and Olkiluoto belongs to the Fennoscandian Shield, one of the ancient continental nuclei of the Earth.

#### 3.1 Forsmark

The current ground surface in the Forsmark region forms a part of the Sub-Cambrian Peneplain in south-eastern Sweden. This peneplain comprises a relatively flat topographic surface with a gentle dip towards the east that formed more than 540 million years ago. The bedrock is covered by a few metres of Quaternary deposits (glacial till mainly) (Figure 3-1). The most elevated areas to the south-west of the candidate area are located at c. 25 m above the Swedish Ordnance Datum RHB 70.

The bedrock at Forsmark formed between 1.89 and 1.85 billion years ago during the Svecokarelian orogeny. It has been affected by both ductile and brittle deformation. The ductile deformation has resulted in large-scale, ductile high-strain belts and more discrete high-strain zones. Tectonic lenses, in which the bedrock is less affected by ductile deformation, are enclosed between the ductile high strain belts (Figure 3-2). The investigation site (candidate area) is located in the north-westernmost part of one of these tectonic lenses. This lens extends from north-west of the nuclear power plant south-eastwards to the area around Öregrund (Figure 3-2). The brittle deformation has given rise to reactivation of the ductile zones in the colder, brittle regime and the formation of new brittle fracture zones of variable size (Figure 3-3).



**Figure 3-1.** Photograph from Forsmark, looking south, showing the flat topography and the low-gradient shoreline with recently isolated bays due to land uplift.



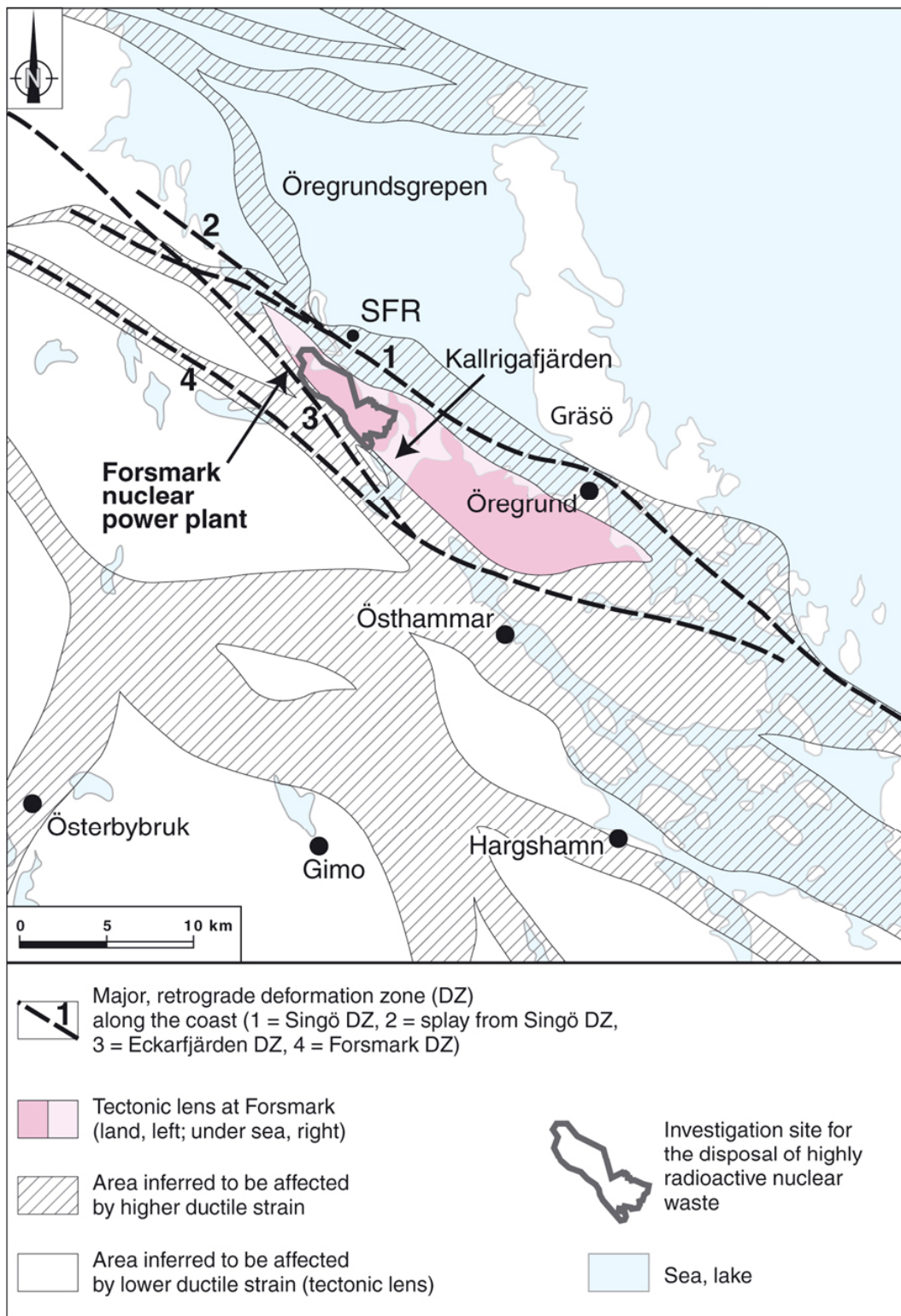


**Figure 3-2.** The tectonic lens at Forsmark and areas affected by strong ductile deformation in the area close to Forsmark.

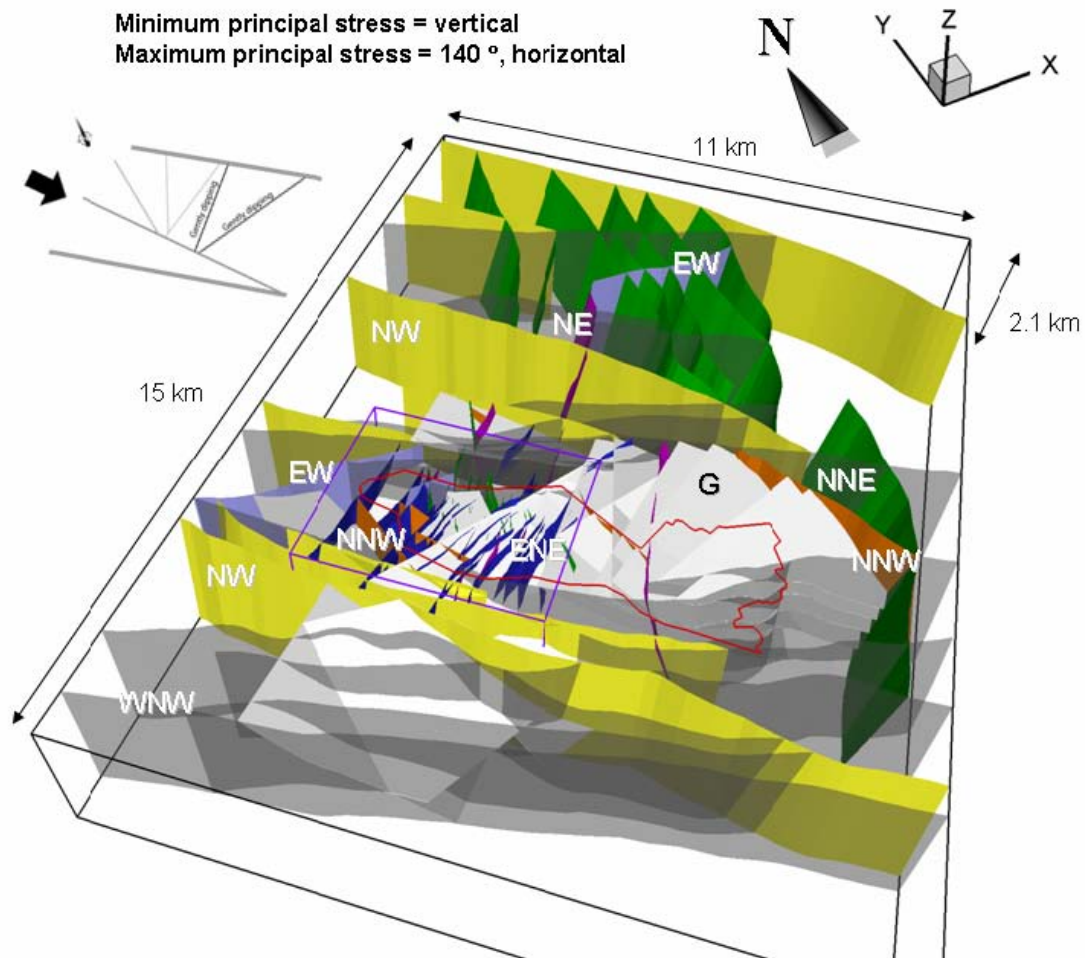


**Figure 3-3.** 3D visualisation of the regional model domain and the 131 deformation zones modelled deterministically at Forsmark. The steeply dipping deformation zones (107) are shaded in different colours and labelled with regard to their principle direction of strike. The gently dipping zones (24) are shaded in pale grey and denoted by a G. The border of the candidate area is shown in red and regional and local model domains in black and purple, respectively. The inset in the upper left corner of the figure shows the direction of the main principal stress.

## 3.2 Laxemar

The investigated area is close to the coast. The topography is fairly flat; the regional topographic gradient is in the order of 4%. The topography corresponds to the Sub-Cambrian Peneplain, but with relatively distinct valleys (Figure 3-4). The Laxemar-Simpevarp regional model area is in general characterised by an undulating bedrock surface with a thin cover of Quaternary deposits, mainly till on the top of the hills and thicker Quaternary deposits in the valleys made up of till overlain by postglacial deposits.



*Figure 3-4. Photograph from the southeast showing the flat topography and near shore situation of the Laxemar-Simpevarp area. The outline of the focused area at Laxemar is shown in red.*

The Laxemar-Simpevarp regional model area is dominated by a geological unit referred to as the Transscandinavian Igneous Belt. The bedrock is dominated by well preserved approximately 1.8 billion years intrusive rocks varying in composition between granite-syenitoid-dioritoid-gabbroid (Figure 3-5). Although a non-uniformly distributed faint to weak foliation, is present, the most prominent ductile structures at Laxemar are discrete, low-temperature, brittle-ductile to ductile shear zones of mesoscopic to regional character, which are related to the waning stages of the Svecokarelian Orogeny. Subsequently, the rock mass has been subjected to repeated phases of brittle deformation, under varying regional stress regimes, involving reactivation along earlier formed structures. There are indications that the ductile anisotropy, including both larger ductile shear zones as well as the weak to faint foliation, minor shear zones and mylonites, has had an influence on the later brittle deformation. With a few exceptions, the deterministically modelled deformation zones at Laxemar are characterised by brittle deformation although virtually all the zones have their origin in an earlier ductile regime. The brittle history of the Laxemar-Simpevarp area is complex and involves a series of reactivation events that do not allow for consistent simple model covering their development (Figure 3-6)

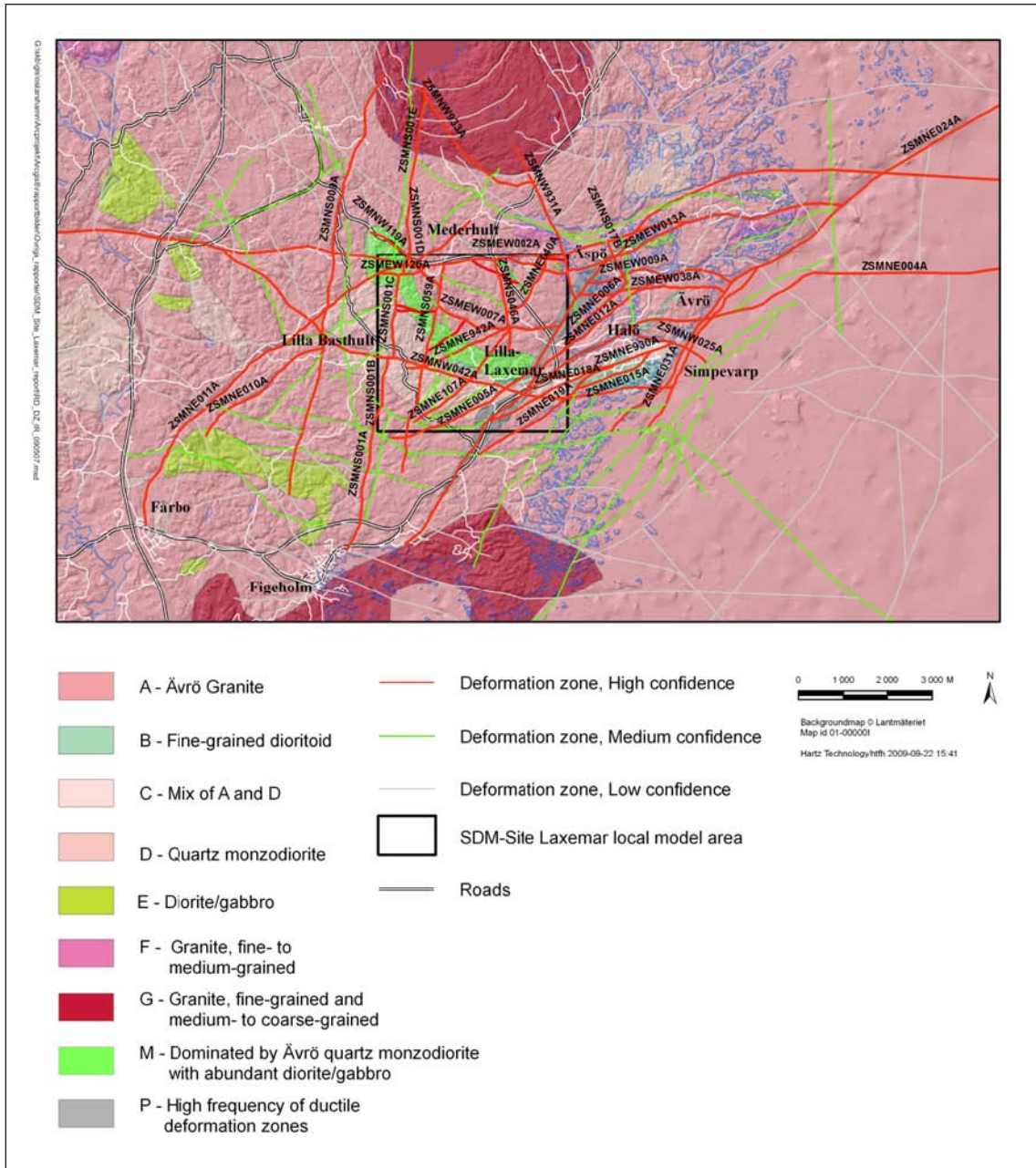


**Figure 3-5.** Major deformation zones and rock domains bounded at Laxemar. The location of the present-day shoreline is indicated by the blue line.

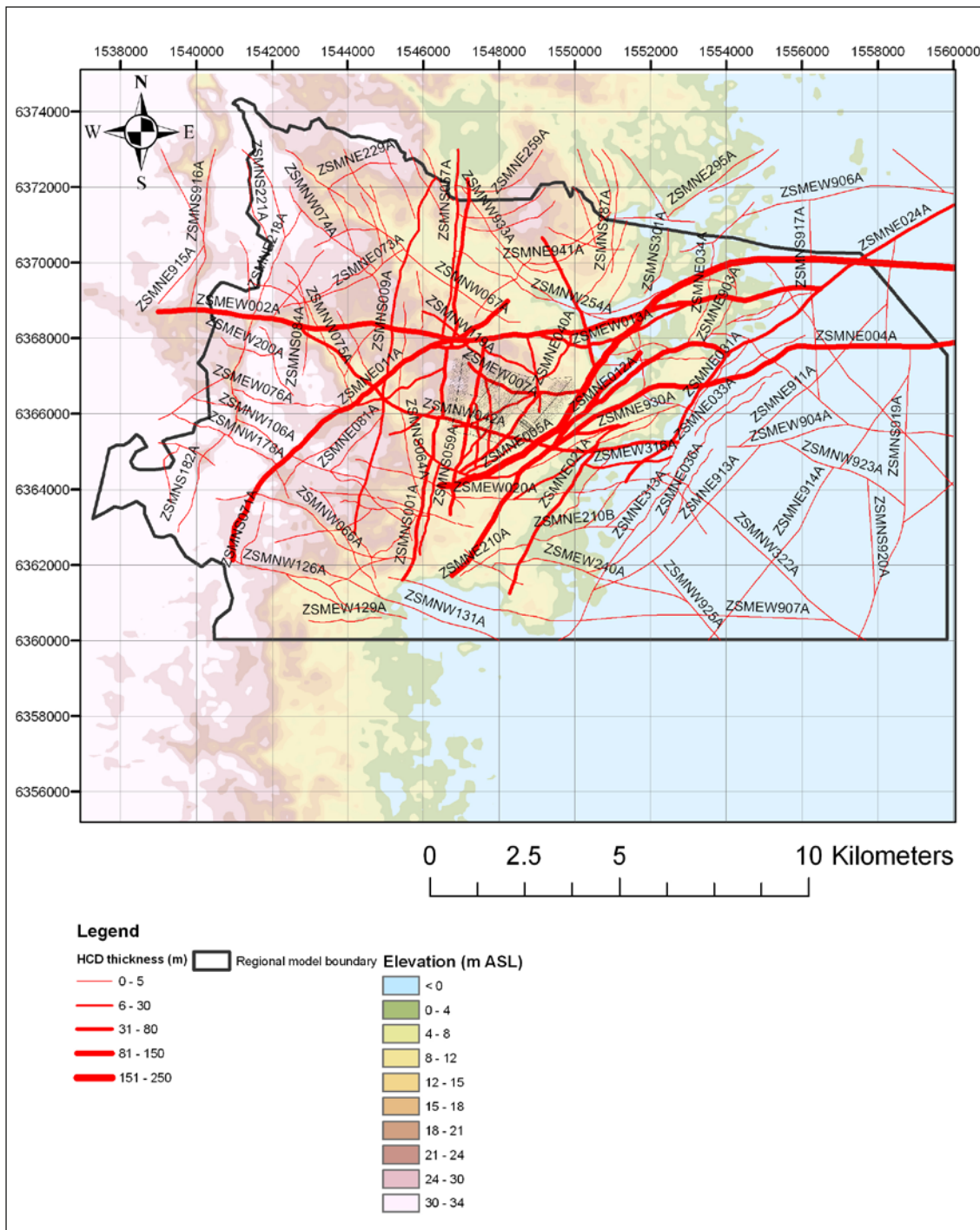


Figure 3-6. Modelled deformation zones at Laxemar. Colouring of zones is according to judged thickness.

### 3.3 Olkiluoto

Olkiluoto is a relatively flat island with an average height of 5 m above sea level, with the highest point at 18 m. The sea area around the island is shallow: mainly less than 12 m within 2 km from the shoreline. The elevations relative to sea level are continuously changing, since the apparent uplift rate is significant at 6 mm/y. The overburden, both onshore and offshore, is usually till.

Olkiluoto is located in the southern part of the Satakunta region where the bedrock displays c. 800 million years of geological history in the Precambrian Fennoscandian Shield. The oldest part of the bedrock consists of supracrustal, metasedimentary and metavolcanic rocks deformed and metamorphosed during the Palaeoproterozoic Svecofennian orogeny c. 1.9–1.8 billion years ago. The rocks are mostly strongly migmatized, high-grade gneisses containing cordierite, sillimanite or garnet porphyroblasts. The supracrustal rocks in Satakunta can be subdivided into two main domains: a pelitic migmatite belt (PEMB) in the southwest and a psammitic migmatite belt (PSMB) in the northeast (Figure 3-7). The pelitic and psammitic migmatite belts can be distinguished on the basis of predominantly granitic and trondhjemitic to granodioritic leucosomes, respectively. Amphibolites, uralite porphyries and hornblende gneisses, which were originally mafic and intermediate volcanic rocks, occasionally occur as narrow interlayers in the supracrustal sequences. Plutonic trondhjemites, tonalites, granodiorites, coarse-grained granites and pegmatites intrude the supracrustal rocks. Except for a few small bodies, more mafic intrusive rocks, gabbros and diorites, are encountered only as small xenoliths.

The geological-tectonic evolution of the bedrock at Olkiluoto reveals a complex geological history, with several phases of deformation (both ductile and brittle) and alteration. The brittle evolution includes several stages of compression and extension, primarily in a NW-SE direction during the period of approximately 1.85–1.1 billion years. Many of the deformation zones at Olkiluoto were formed during this period, and this was followed by fault reactivation and some uplift 900–600 million years ago, platform sedimentation (600–240 million years), and the Caledonian foreland stage (420–350 million years). More importantly, however, is the opening of the north Atlantic Ocean (and the associated mid-Atlantic ridge) and the uplift of western Scandinavia, both of which commenced during the Eocene and Oligocene (starting approximately 55 million years ago), as these represent the most recent and current major tectonic events, with what is termed ‘ridge push’ from the opening of the Atlantic Ocean being still active.

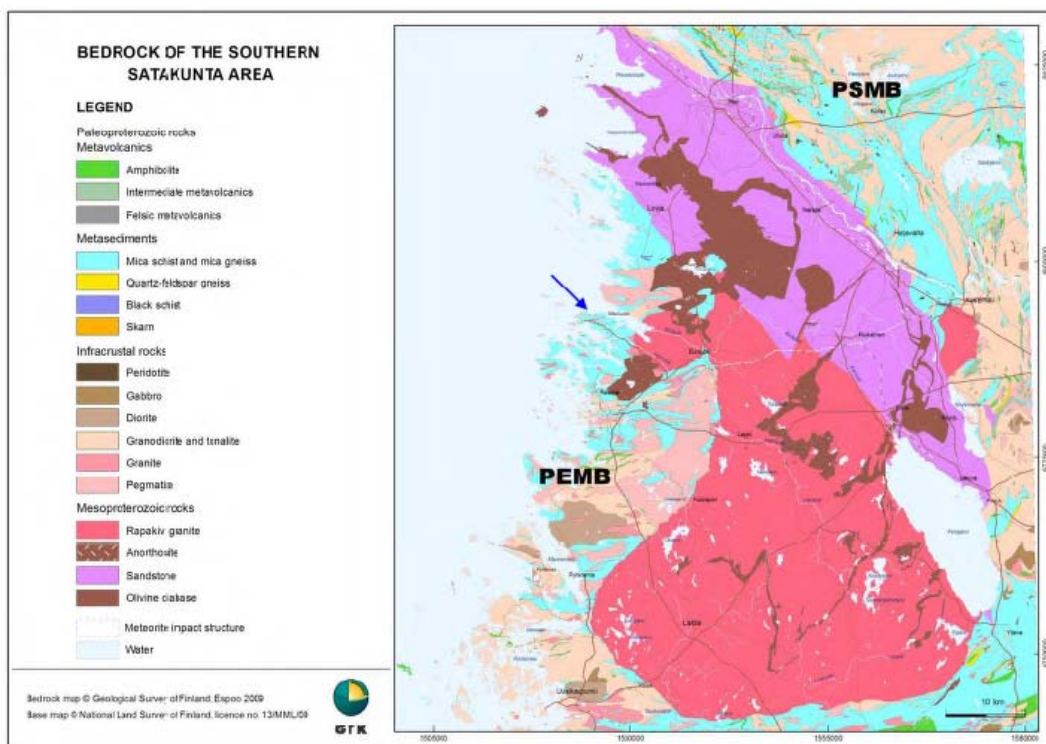


**Figure 3-7.** Regional geology in the vicinity of the Olkiluoto area. Olkiluoto Island is marked by a blue arrow. PEMB = pelitic migmatite belt, PSMB = psammitic migmatite belt (see text).

Figure 3-8 shows the interpreted brittle deformation zones at the depth of 0 m on the map of Olkiluoto and shows them, together with the lithology, along a N-S trending section (X = 1526000) (Figure 3-9). A large number of the brittle deformation zones are gently dipping.

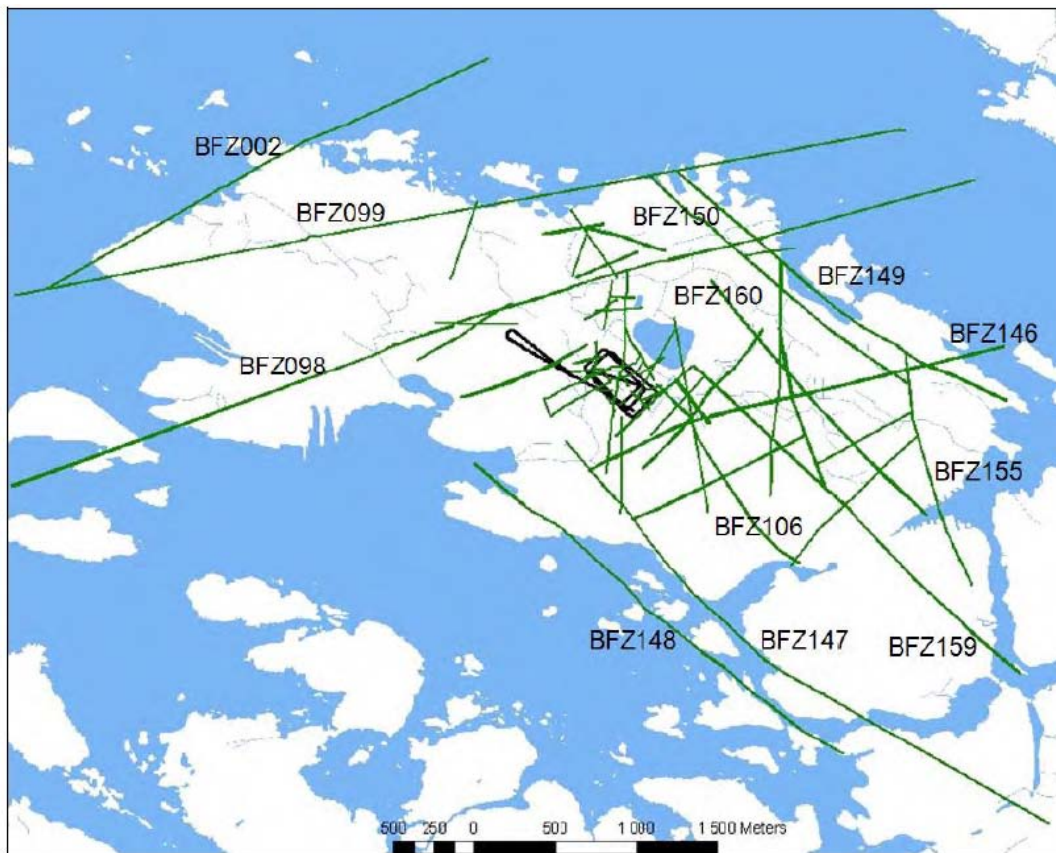


**Figure 3-8.** Modelled brittle deformation zones at  $Z = 0$  (green lines). The site-scale zones are labelled. The location of the ONKALO facility is shown in the centre.

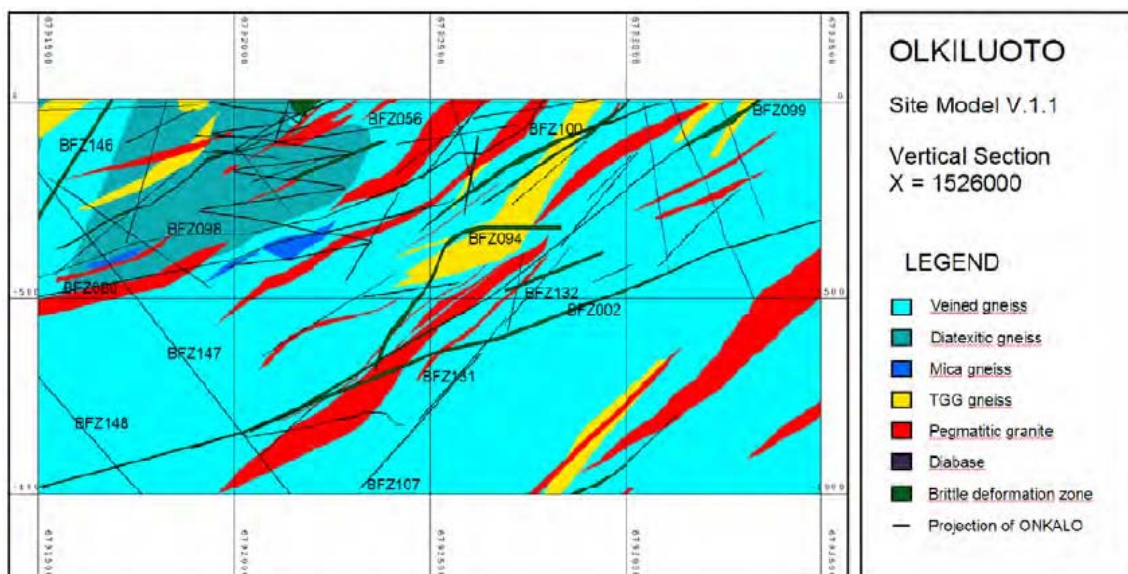


**Figure 3-9.** Modelled brittle deformation zones with lithology, N-S trending vertical section ( $X = 1526000$ ). View from the east.

## 4 Hydrogeological properties – Forsmark

### 4.1 Main hydraulic characteristics

The deepest boreholes at Forsmark reach –1,000 m elevation. Field measurements suggest that the value of the hydraulic diffusivity in the bedrock is locally very high, particularly in the upper c. 150 m of bedrock where large sheet joints and gently dipping deformation zones cuts through the rock mass volumes between steeply dipping deformation zones. High transmissivities and low specific storages in shallow, brittle structures imply little or no delay in hydraulic responses to different kinds of pressure disturbances in the uppermost 150 m of bedrock. Notably, below –400 m elevation, the rock mass volumes between deformation zones is close to the percolation threshold.

There are both gently dipping and steeply dipping deformation zones at Forsmark. However, field studies suggest that the hydraulically most important deformation zones inside the tectonic lens are gently dipping.

### 4.2 Deformation zones

#### 4.2.1 Transmissivity

An exponential trend model for the depth dependency of the in-plane deformation zone transmissivity  $T$  [ $L^2T^{-1}$ ;  $m^2/s$ ] is suggested:

$$T(z) = \max \begin{cases} T(0) 10^{z/k} \\ 1 \cdot 10^{-9} \end{cases} \quad (4-1)$$

where  $T(z)$  is the in-plane deformation zone transmissivity,  $z$  [L; m] is the elevation relative to the sea level,  $T(0)$  is the value of the transmissivity of the deformation zone at zero elevation, and  $k$  [L; m] is the depth interval that gives an order of magnitude decrease in transmissivity. The following values of  $T(0)$  and  $k$  are suggested:

$$T_{ENE}(0) = 2.5 \cdot 10^{-7} \text{ m}^2/\text{s}$$

$$T_{NE}(0) = 3.4 \cdot 10^{-7} \text{ m}^2/\text{s}$$

$$T_{NNE}(0) = 1.5 \cdot 10^{-6} \text{ m}^2/\text{s}$$

$$T_{NNW}(0) = 9.3 \cdot 10^{-7} \text{ m}^2/\text{s}$$

$$T_{NW}(0) = 2.1 \cdot 10^{-5} \text{ m}^2/\text{s}$$

$$T_{WNW}(0) = 2.8 \cdot 10^{-5} \text{ m}^2/\text{s}$$

$$T_G(0) = 2.2 \cdot 10^{-4} \text{ m}^2/\text{s}$$

$$k = 232.5 \text{ m}$$

Lateral in-plane heterogeneity is simulated by adding a log-normal random deviate to the exponent in Equation 4-1:

$$T(z) = \max \begin{cases} T(0) 10^{z/k + N(0, s_{\log(T)})} \\ 1 \cdot 10^{-9} \end{cases} \quad (4-2)$$

where  $s_{\log(T)} = 0.632$ . This value of  $s_{\log(T)}$  implies that the range of the 95% confidence interval for a new transmissivity observation is approximately 2.5 orders of magnitude.



## 4.2.2 Stresses

*In-situ* stress gradients versus depth at Forsmark are given in Table 4-1 and Figure 4-1.

Table 4-1 implies that the gently dipping deformation zones are at a high angle to the minimum principal stress ( $\sigma_{3v}$ ) and at a low angle to the azimuths of both the first ( $\sigma_{1H}$ ) and second principal stresses ( $\sigma_{2h}$ ). Further, the deformation zones that strike WNW-NW are at low angle to the azimuth of  $\sigma_{1H}$ , whereas the opposite condition prevails for the deformation zones that strike NNE-ESE. The observation made at Forsmark is that the former set of zones is more transmissive than the latter set. The most transmissive set of zones is however the gently dipping.

**Table 4-1. Recommended horizontal and vertical stress magnitudes for the Forsmark target area, where the depth below surface is  $d$  in metres. A depth of 0 is approximately equal to an elevation of 0 m.**

Depth [m]	Maximum horizontal stress, $\sigma_{1H}$ [MPa]	Trend [°]	Minimum horizontal stress, $\sigma_{2h}$ [MPa]	Trend [°]	Vertical stress $\sigma_{3v}$ [MPa]
0–150	$19+0.008d \pm 20\%$	$145 \pm 20$	$11+0.006d \pm 25\%$	055	$0.0265d \pm 2\%$
150–400	$9.1+0.074d \pm 15\%$	$145 \pm 15$	$6.8+0.034d \pm 25\%$	055	$0.0265d \pm 2\%$
400–600	$29.5+0.023d \pm 15\%$	$145 \pm 15$	$9.2+0.028d \pm 20\%$	055	$0.0265d \pm 2\%$

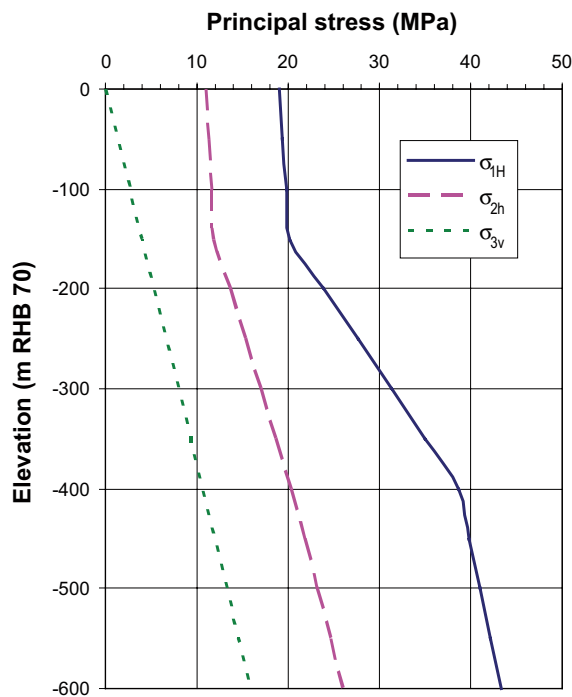


**Figure 4-1.** Plot of the recommended in-situ stress gradients versus depth at Forsmark.  $\sigma_{1H}$  = Maximum horizontal stress,  $\sigma_{2h}$  = minimum horizontal stress and  $\sigma_{3v}$  = vertical stress. All principal stresses increase with depth.

## 4.3 Rock mass volumes between deformation zones

### 4.3.1 DFN properties

Table 4-2 shows the suggested DFN properties between ground surface and –1,000 m elevation. In this table,  $P_{32,open}$  [ $L^{-1}$ ;  $m^2/m^3$ ] represents the open fracture surface area per unit volume of rock.  $P_{32,open}$  is estimated from the Terzaghi corrected linear frequencies of observed open fractures,  $P_{10,open,corr}$ . Further, parameter values for a semi-correlated fracture transmissivity models are given. For elevations below –1,000 m elevation, continuum properties are suggested, see Section 4.3.3.

### 4.3.2 ECPM properties

Equivalent continuous porous medium (ECPM) properties are obtained by means of up-scaling each fracture network (DZ and DFN) realisation generated. See Section 4.3.1 for a specification of DFN properties.

### 4.3.3 CPM and SC properties

Table 4-3 shows continuum properties derived from double-packer injection tests conducted on a 100-m scale. For CPM modelling, the values of average  $\log(K)$  values with depth are suggested as points for regression. This allows the user to match a continuous function from which grid properties may be derived. For SC modelling, the different standard deviations of  $\log(K)$  are used as normal random deviates and added to the average  $\log(K)$  values.

For the sake of comparison, Table 4-4 shows continuum properties estimated from the conductive fracture frequency ( $m^{-1}$ ) and the specific capacity ( $m^2/s$ ) of flowing fractures identified with the Posiva Flow Log. Note that the median block size varies with depth Table 4-4. CPM and SC properties derived from Table 4-4 should be handled with care.

**Table 4-2. Suggested statistical distributions and parameter values for DFN modelling. Note that the minimum and maximum radii of the stochastically generated structures are 0.038 m and 564 m, respectively.**

Elevation [m RHB 70]	Set name	Orientation poles: Fisher (trend, plunge), conc. $\kappa$ [°, °, –]	Size model, power-law ( $r_0, k_r$ ) [m, –]	Intensity, ( $P_{32,open}$ ), valid size interval: ( $r_0, 564$ m) [ $m^2/m^3$ ]	Semi-correlated transmissivity model $\log(T) = \log(a r^{-b}) + s_{\log(T)} N(0,1)$ ( $a, b, \sigma_{\log T}$ )
> –200	NS	(292, 1) 17.8	(0.038, 2.75)	0.497	(9.0·10 <sup>-9</sup> , 0.7, 1.0)
	NE	(326, 2) 14.3	(0.038, 2.62)	0.533	
	NW	(60, 6) 12.9	(0.038, 3.20)	0.326	
	EW	(15, 2) 14.0	(0.038, 3.40)	0.116	
	HZ	(5, 86) 15.2	(0.038, 2.58)	1.609	
–200 to –400	NS	As above	As above	0.229	(1.3·10 <sup>-9</sup> , 0.5, 1.0)
	NE	As above	As above	0.432	
	NW	As above	As above	0.135	
	EW	As above	As above	0.105	
	HZ	As above	As above	0.331	
< –400 to –1,000	NS	As above	As above	0.122	(5.3·10 <sup>-11</sup> , 0.5, 1.0)
	NE	As above	As above	0.193	
	NW	As above	As above	0.100	
	EW	As above	As above	0.056	
	HZ	As above	As above	0.158	

**Table 4-3. CPM and SC properties derived from double-packer injection tests conducted on a 100-m scale. Values shown between parentheses are optional.**

Elevation	Median Block size	Average log( <i>K</i> )	Std dev log( <i>K</i> )	Variogram model	Correlation length
[m RHB 70]	[m]	<i>K</i> in [m/s]	<i>K</i> in [m/s]	[-]	$\lambda$ in [m]
> -200	100	-8.63	1.44	Nugget	Grid size
-200 to -400	100	-10.5	1.07	Nugget	Grid size
-400 to -1,000 (-5,000)	100	-11.0	1.12	Nugget	Grid size

**Table 4-4. CPM and SC properties derived from derived from the conductive fracture frequency ( $m^{-1}$ ) and the specific capacity ( $m^2/s$ ) of flowing fractures identified with the Posiva Flow Log. Values shown between parentheses are optional.**

Elevation	Median Block size	Average log( <i>K</i> )	Std dev log( <i>K</i> )	Variogram model	Correlation length
[m RHB 70]	[m]	<i>K</i> in [m/s]	<i>K</i> in [m/s]	[-]	$\lambda$ in [m]
> -200	3 (3.33)	-8.49	1.15	Nugget (Exponential)	Grid size (200)
-200 to -400	24 (25)	-9.90	0.75	Nugget (Exponential)	Grid size (200)
< -400 to -1,000 (-5,000)	200 (100)	-10.49	0.55	Nugget	Grid size

## 5 Hydrogeological properties – Laxemar

### 5.1 Main hydraulic characteristics

Investigations have essentially been made down to approximately 1,000 m depth but there is also one borehole (KLX02) that has provided data down to c. 1,600 m depth. The crystalline bedrock is intersected by a number of deformation zones which are mainly steeply dipping. Hydraulically, the deformation zones are generally more conductive than the rock mass volumes in between. The general tendency within the Laxemar-Simpevarp regional model volume is that the hydraulic conductivity decreases with depth although the lateral heterogeneity at all elevations is large.

### 5.2 Deformation zones

#### 5.2.1 Transmissivity

An exponential trend model for the depth dependency of the in-plane deformation zone transmissivity  $T$  [ $L^2T^{-1}$ ;  $m^2/s$ ] is suggested:

$$T(z) = \max \begin{cases} T(0) 10^{z/k} \\ 1 \cdot 10^{-9} \end{cases} \quad (5-1)$$

where  $T(z)$  is the in-plane deformation zone transmissivity,  $z$  [L; m] is the elevation relative to the sea level,  $T(0)$  is the value of the transmissivity of the deformation zone at zero elevation, and  $k$  [L; m] is the depth interval that gives an order of magnitude decrease in transmissivity. The following values of  $T(0)$  and  $k$  are suggested:

$$L < 2 \text{ km: } T_{EW}(0) = 2.2 \cdot 10^{-5} \text{ m}^2/\text{s} ; k = 380.2 \text{ m}$$

$$L > 2 \text{ km: } T_{EW}(0) = 8.1 \cdot 10^{-5} \text{ m}^2/\text{s} ; k = 534.8 \text{ m}$$

$$L < 2 \text{ km: } T_{NW}(0) = 1.0 \cdot 10^{-5} \text{ m}^2/\text{s} ; k = 400.0 \text{ m}$$

$$L > 2 \text{ km: } T_{NW}(0) = 8.5 \cdot 10^{-5} \text{ m}^2/\text{s} ; k = 365.0 \text{ m}$$

$$L < 2 \text{ km: } T_{NS}(0) = 1.0 \cdot 10^{-5} \text{ m}^2/\text{s} ; k = 400.0 \text{ m}$$

$$L > 2 \text{ km: } T_{NS}(0) = 8.5 \cdot 10^{-5} \text{ m}^2/\text{s} ; k = 365.0 \text{ m}$$

$$L < 2 \text{ km: } T_{NE}(0) = 1.0 \cdot 10^{-5} \text{ m}^2/\text{s} ; k = 400.0 \text{ m}$$

$$L > 2 \text{ km: } T_{NE}(0) = 8.5 \cdot 10^{-5} \text{ m}^2/\text{s} ; k = 365.0 \text{ m}$$

Lateral in-plane heterogeneity is simulated by adding a log-normal random deviate to the exponent in Equation 5-1:

$$T(z) = \max \begin{cases} T(0) 10^{z/k + N(0, s_{\log(T)})} \\ 1 \cdot 10^{-9} \end{cases} \quad (5-2)$$

where  $s_{\log(T)} = 1.35$ . This value of  $s_{\log(T)}$  implies that the 95% confidence interval in the lateral spread in  $\log(T)$  is approximately 5.3 orders of magnitude.

#### 5.2.2 Stresses

The rock mechanics model for SDM-Site Laxemar indicates that the present orientation of the maximum principal horizontal stress is WNW-ESE, which corresponds well to the E-W deformation zones being the most transmissive.

## 5.3 Rock mass volumes between deformation zones

### 5.3.1 DFN properties

Table 5-1 shows the suggested DFN properties between ground surface and –1,000 m elevation. In this table,  $P_{32,open}$  [ $L^{-1}$ ;  $m^2/m^3$ ] represents the open fracture surface area per unit volume of rock.  $P_{32,open}$  is estimated from the Terzaghi corrected linear frequencies of observed open fractures,  $P_{10,open,corr}$ . Further, parameter values for a semi-correlated fracture transmissivity models are given. For elevations below –1,000 m elevation, continuum properties are suggested, see Section 4.3.3.

### 5.3.2 ECPM properties

Equivalent continuous porous medium (ECPM) properties are obtained by means of up-scaling each fracture network (DZ and DFN) realisation generated. See Sections 4.3.1 for the specification of DFN properties.

### 5.3.3 CPM and SC properties

Table 5-2 shows continuum properties derived from double-packer injection tests conducted on a 100-m scale. For CPM modelling, the values of average  $\log(K)$  values with depth are suggested as points for regression. This allows the user to match a continuous function from which grid properties may be derived. For SC modelling, the different standard deviations of  $\log(K)$  are used as normal random deviates and added to the average  $\log(K)$  values.

For the sake of comparison, Table 5-3 shows continuum properties estimated from the conductive fracture frequency ( $m^{-1}$ ) and the specific capacity ( $m^2/s$ ) of flowing fractures identified with the Posiva Flow Log. Note that the median block size varies with depth Table 5-3. CPM and SC properties derived from Table 5-3 should be handled with care.

**Table 5-1. Suggested statistical distributions and parameter values for DFN modelling. Note that the minimum and maximum radii of the stochastically generated structures are 0.038 m and 564 m, respectively.**

Elevation [m RHB 70]	Set name	Orientation poles: Fisher (trend, plunge), conc. $\kappa$ [°, °, –]	Size model, power-law ( $r_0$ , $k_r$ ) [m, –]	Intensity, ( $P_{32,open}$ ), valid size interval: ( $r_0$ , 564 m) [ $m^2/m^3$ ]	Semi-correlated transmissivity model $\log(T) = \log(a r^b) + s_{\log(T)} N(0,1)$ ( $a, b, \sigma_{\log T}$ )
> –150	ENE	(155.1, 3.4) 9.6	(0.038, 2.70)	0.52	( $2 \cdot 10^{-7}$ , 0.7, 0.4)
	WNW	(204, 1.6) 12.0	(0.038, 2.49)	0.95	( $2 \cdot 10^{-7}$ , 0.9, 0.6)
	NS	(270.2, 8.4) 7.8	(0.038, 2.80)	0.54	( $8 \cdot 10^{-8}$ , 0.5, 0.4)
	SubH	(46.3, 84.7) 12.0	(0.038, 2.59)	1.20	( $6 \cdot 10^{-8}$ , 0.7, 0.5)
–150 to –400	ENE	As above	(0.038, 3.00)	0.47	( $6 \cdot 10^{-7}$ , 0.7, 0.9)
	WNW	As above	(0.038, 2.44)	0.55	( $1 \cdot 10^{-8}$ , 0.5, 0.7)
	NS	As above	(0.038, 2.91)	0.63	( $1 \cdot 10^{-8}$ , 0.7, 0.2)
	SubH	As above	(0.038, 2.87)	0.71	( $3.5 \cdot 10^{-8}$ , 1.2, 0.9)
–400 to –650	ENE	As above	(0.038, 2.87)	0.38	( $8 \cdot 10^{-8}$ , 0.8, 0.6)
	WNW	As above	(0.038, 2.54)	0.74	( $3 \cdot 10^{-9}$ , 0.8, 0.6)
	NS	As above	(0.038, 2.87)	0.47	( $6 \cdot 10^{-9}$ , 0.4, 0.4)
	SubH	As above	(0.038, 3.00)	0.58	( $2 \cdot 10^{-7}$ , 0.8, 0.7)
–650 to –1,000	ENE	As above	(0.038, 2.96)	0.46	( $1 \cdot 10^{-8}$ , 0.7, 0.4)
	WNW	As above	(0.038, 3.00)	0.73	( $3 \cdot 10^{-7}$ , 0.7, 0.4)
	NS	As above	(0.038, 3.00)	0.25	( $1 \cdot 10^{-8}$ , 0.7, 0.4)
	SubH	As above	(0.038, 2.97)	0.35	( $1 \cdot 10^{-7}$ , 0.7, 0.4)

**Table 5-2. CPM and SC properties derived form double-packer injection tests conducted on a 100-m scale.**

Elevation [m RHB 70]	Average log( <i>K</i> ) <i>K</i> in [m/s]	Std dev log( <i>K</i> ) <i>K</i> in [m/s]	Variogram model [-]	Correlation length $\lambda$ in [m]
+50 to -150	-6.96	1.04	Nugget	Grid size
-150 to -400	-7.81	1.63	Nugget	Grid size
-400 to -650	-9.05	1.78	Nugget	Grid size
< -650 to -1,000 (-5,000)	-9.66	1.70	Nugget	Grid size

**Table 5-3. CPM and SC properties derived from derived from the conductive fracture frequency ( $m^{-1}$ ) and the specific capacity ( $m^2/s$ ) of flowing fractures identified with the Posiva Flow Log. Values shown between parentheses are optional.**

Elevation [m RHB 70]	Median Block size [m]	Average log( <i>K</i> ) <i>K</i> in [m/s]	Std dev log( <i>K</i> ) <i>K</i> in [m/s]	Variogram model [-]	Correlation length $\lambda$ in [m]
+50 to -150	2	-7.22	1.27	Nugget (Exponential)	Grid size (200)
-150 to -400	6 (5)	-7.95	1.15	Nugget (Exponential)	Grid size (200)
-400 to -650	10	-8.72	0.90	Nugget (Exponential)	Grid size (200)
< -650 to -1,000 (-5,000)	125 (100)	-9.69	0.63	Nugget	Grid size

## 6 Hydrogeological properties – Olkiluoto

### 6.1 Main hydraulic characteristics

Field studies suggest that the hydraulically most important deformation zones in the Olkiluoto site area are gently dipping; fourteen out of fifteen so-called hydro-zones are gently dipping, the average strike of which is  $143^\circ$  (range  $118^\circ$ – $169^\circ$ ) and the average dip is  $18^\circ$  (range  $5^\circ$ – $33^\circ$ ). However, there is no particular geometrical criterion of what characterises a hydro-zone; i.e., the criterion is purely hydraulic. For instance, all transmissivities greater than  $1 \cdot 10^{-5}$  m<sup>2</sup>/s are modelled deterministically as hydro-zones. In comparison, steeply dipping deformations have significantly less transmissivity.

### 6.2 Hydro-zones

#### 6.2.1 Transmissivity based on injections tests and pumping tests

Based on injections tests and pumping tests, univariate statistics of the hydro-zone transmissivity are reported. Notably, there are two references available and none of these suggest a depth dependence. On the average, the following hydraulic properties are suggested for the gently dipping hydro-zones:

##### **Study 1 /Ahokas et al. 2007/**

Average  $\log(T)$  =  $-6.24$  (i.e., a geometric mean of  $5.7 \cdot 10^{-7}$  m<sup>2</sup>/s)

Std dev  $\log(T)$  =  $1.22$

Max  $\log(T)$  =  $-3.84$  (i.e.,  $1.4 \cdot 10^{-4}$  m<sup>2</sup>/s)

Min  $\log(T)$  =  $-8.63$  (i.e.,  $2.3 \cdot 10^{-9}$  m<sup>2</sup>/s)

The value of  $s_{\log(T)} = 1.22$  implies that the range of the 95% confidence interval for a new transmissivity observation is approximately 4.8 orders of magnitude.

##### **Study 2 /Vaittinen et al. 2009/**

Average  $\log(T)$  =  $-6.00$  (i.e., a geometric mean of  $1.0 \cdot 10^{-6}$  m<sup>2</sup>/s)

Std dev  $\log(T)$  =  $0.84$

Max  $\log(T)$  =  $-4.35$  (i.e.,  $4.4 \cdot 10^{-5}$  m<sup>2</sup>/s)

Min  $\log(T)$  =  $-7.64$  (i.e.,  $2.3 \cdot 10^{-8}$  m<sup>2</sup>/s)

The value of  $s_{\log(T)} = 0.84$  implies that the range of the 95% confidence interval for a new transmissivity observation is approximately 3.3 orders of magnitude.

#### 6.2.2 Transmissivity based on difference flow logging

Based on the conductive fracture frequency (m<sup>-1</sup>) and the specific capacity (m<sup>2</sup>/s) of flowing fractures identified with the Posiva Flow Log, an exponential trend model for the depth dependency of the in-plane hydro-zone transmissivity  $T$  [L<sup>2</sup>T<sup>-1</sup>; m<sup>2</sup>/s] may be suggested:

$$T(z) = \begin{cases} T_1(0) 10^{z/k_1}, & z > -500 \\ T_2(0) 10^{z/k_2}, & -500 > z > -700 \\ 1 \cdot 10^{-9}, & z < -700 \end{cases} \quad (6-1)$$

where  $T(z)$  is the in-plane hydro-zone transmissivity,  $z$  [L; m] is the elevation relative to the sea level,  $T(0)$  is the value of the trend model transmissivity at zero elevation, and  $k$  [L; m] is the depth interval that gives an order of magnitude decrease in transmissivity. Here, the following values of  $T(0)$  and  $k$  are suggested:

$$\begin{aligned} T_1(0) &= 2.5 \cdot 10^{-4} \text{ m}^2/\text{s}, z < -500 \\ T_2(0) &= 5.0 \cdot 10^{-2} \text{ m}^2/\text{s}, -500 > z > -700 \\ k_1 &= 185.3 \text{ m} \\ k_2 &= 100.0 \text{ m} \end{aligned}$$

Lateral in-plane heterogeneity may be simulated by adding a log-normal random deviate to the exponent in Equation 6-1:

$$T(z) = \begin{cases} T_1(0) 10^{z/k_1 + N(0, s_{\log(T)})}, & z > -500 \\ T_2(0) 10^{z/k_2 + N(0, s_{\log(T)})}, & -500 > z > -700 \\ 1 \cdot 10^{-9}, & z < -700 \end{cases} \quad (6-2)$$

where  $s_{\log(T)} = 1.22$  (Model 1) or  $0.84$  (Model 2) according to Section 5.2.1. The corresponding minimum and maximum values are also specified in Section 5.2.1.

### 6.2.3 Stresses

In summary, the following conclusions can be stated regarding the *in situ* state of stress at Olkiluoto:

- A thrust faulting stress regime applies, i.e.,  $\sigma_H > \sigma_h > \sigma_v$ . Also, the principal stresses are oriented horizontally and vertically, respectively. In the stress model, the vertical stress is taken to be equal to the overburden stress, with an assumed variation of 10%.
- On the regional scale, the maximum horizontal stress component is oriented NW-SE ( $146^\circ$  as inferred from relative plate motions) but the data suggest a maximum horizontal stress orientation of N-S for the upper portion of the rock mass (0–300 m) and E-W for the lower portion of the rock mass (300–900 m).
- For the maximum and minimum horizontal stress, a bi-linear stress model is proposed, per the above. For a repository target depth of 450 m, the mean stresses and estimated lower and upper limits (corresponding to the 10th and 90th percentiles) are estimated as:  $\sigma_H = 27$  (21–33) MPa,  $\sigma_h = 16$  (12–20) MPa, and  $\sigma_v = 12$  (11–13) MPa.

## 6.3 Rock mass volumes between deformation zones

### 6.3.1 DFN properties

Table 6-1 shows the suggested DFN properties between ground surface and  $-1,000$  m elevation. In this table,  $P_{32,open}$  [ $L^{-1}$ ;  $m^2/m^3$ ] represents the open fracture surface area per unit volume of rock.  $P_{32,open}$  is estimated from the Terzaghi corrected linear frequencies of observed open fractures,  $P_{10,open,corr}$ . Further, parameter values for a semi-correlated fracture transmissivity models are given. For elevations below  $-1,000$  m elevation, continuum properties are suggested, see Section 6.3.3.

### 6.3.2 ECPM properties

Equivalent continuous porous medium (ECPM) properties are obtained by means of up-scaling each fracture network (DZ and DFN) realisation generated. See Section 6.3.1 for a specification of DFN properties.



**Table 6-1. Suggested statistical distributions and parameter values for DFN modelling. Note that the minimum and maximum radii of the stochastically generated structures are 0.038 m and 564 m, respectively.**

Elevation [m RHB 70]	Set name	Orientation poles: Fisher (trend, plunge), conc. $\kappa$ [°, °, -]	Size model, power-law ( $r_0, k_r$ ) [m, -]	Intensity, ( $P_{32,open}$ ), valid size interval: ( $r_0, 564$ m) [m <sup>2</sup> /m <sup>3</sup> ]	Semi-correlated transmissivity model $\log(T) = \log(a r^b) + s_{\log(T)} N(0,1)$ ( $a, b, \sigma_{\log T}$ ) =
> -50	EW	(185, 5) 10.4	(0.038, 2.50)	0.44	( $6 \cdot 10^{-8}$ , 0.7, 0.8)
	NS	(91, 8) 8.1	(0.038, 2.50)	0.40	( $6 \cdot 10^{-8}$ , 0.7, 0.7)
	HZ	(301, 85) 6.1	(0.038, 2.60)	1.96	( $1.8 \cdot 10^{-7}$ , 0.7, 0.8)
-50 to -150	EW	(185, 5) 10.4	(0.038, 2.60)	0.50	( $1 \cdot 10^{-8}$ , 0.7, 0.7)
	NS	(91, 8) 8.1	(0.038, 2.60)	0.49	( $1 \cdot 10^{-8}$ , 0.7, 0.7)
	HZ	(301, 85) 6.1	(0.038, 2.7)	1.61	( $3 \cdot 10^{-8}$ , 0.7, 0.7)
-150 to -400	EW	(185, 5) 10.4	(0.038, 2.65)	0.44	( $2.2 \cdot 10^{-9}$ , 0.7, 0.7)
	NS	(91, 8) 8.1	(0.038, 2.65)	0.40	( $2.2 \cdot 10^{-9}$ , 0.7, 0.7)
	HZ	(301, 85) 6.1	(0.038, 2.65)	1.96	( $7 \cdot 10^{-9}$ , 1.1, 0.7)
< -400 to -1,000	EW	(185, 5) 10.4	(0.038, 2.50)	0.44	( $5 \cdot 10^{-10}$ , 0.7, 0.7)
	NS	(91, 8) 8.1	(0.038, 2.50)	0.40	( $5 \cdot 10^{-10}$ , 0.7, 0.7)
	HZ	(301, 85) 6.1	(0.038, 2.6)	1.96	( $1.5 \cdot 10^{-9}$ , 1.1, 0.7)

### 6.3.3 CPM and SC properties

Table 6-2 shows suggested continuum properties derived from the conductive fracture frequency ( $m^{-1}$ ) and the specific capacity ( $m^2/s$ ) of flowing fractures identified with the Posiva Flow Log.

For CPM modelling, the values of average  $\log(K)$  values with depth are suggested as points for regression. This allows the user to match a continuous function from which grid properties may be derived. For SC modelling, the different standard deviations of  $\log(K)$  are used as normal random deviates and added to the average  $\log(K)$  values. Autocorrelation may be excluded or included as indicated in Table 6-2.

**Table 6-2. CPM and SC properties derived from the conductive fracture frequency and the specific capacity of flowing fractures identified with the Posiva Flow Log. Values shown between parentheses are optional.**

Elevation [m RHB 70]	Median Block size [m]	Average $\log(K)$ $K$ in [m/s]	Std dev $\log(K)$ $K$ in [m/s]	Variogram model [-]	Correlation length $\lambda$ in [m]
> -100	4	-9.00	0.90	Nugget (Exponential)	Grid size (100)
-100 to -200	20	-9.15	0.74	Nugget (Exponential)	Grid size (100)
-200 to -400	30 (33.3)	-9.40	0.74	Nugget (Exponential)	Grid size (100)
< -400 to -1,000 (-5,000)	70 (100)	-10.04	0.74	Nugget	Grid size

## 7 Storage and transport properties

### 7.1 Specific storage and storativity

Specific storage is important in transient flow problems. In terms of measurable physical properties, volumetric specific storage  $S_s$  [ $L^{-1}$ ;  $m^{-1}$ ] can be expressed as:

$$S_s = \gamma (\alpha + \phi\beta) \quad (7-1)$$

where  $\gamma$  [ $ML^{-2}T^{-2}$ ;  $N/m^3$ ] is the specific weight of water,  $\alpha$  [ $LM^{-1}T^2$ ;  $m^2/N$ ] is the compressibility of the saturated porous medium,  $\phi$  [-] is the kinematic porosity of the saturated porous medium, and  $\beta$  [ $LM^{-1}T^2$ ;  $m^2/N$ ] is the compressibility of water. In discrete fracture network models, values of specific storage are assigned to each fracture and deformation zone. Hence, each structure is treated as a saturated porous medium with a storativity  $S$  [-] defined as:

$$S = S_s B \quad (7-2)$$

where  $B$  [ $L$ ;  $m$ ] is the geological width (thickness) of the structure.

The hydraulic interference tests conducted in conjunction with investigations for the construction of the Äspö HRL suggest a power law relationship between the storativity and transmissivity:

$$S = a T^b \quad (7-3)$$

where  $a = 0.00922$  and  $b = 0.789$ . It is assumed here that Equation 7-3 is valid also at Forsmark, Laxemar and Olkiluoto, with the same values of  $a$  and  $b$  as at the Äspö HRL. However, at Forsmark it is suggested that a ten times smaller value of  $a$  is used based on the high hydraulic diffusivity observed, i.e.,  $a = 0.000922$ .

### 7.2 Kinematic porosity

Kinematic porosity  $\phi$  [-] is to some extent coupled to hydraulic conductivity. Sometimes the following equation is used:

$$\phi(K) = a K^b \quad (7-4)$$

where  $a = 34.87$ ,  $b = 0.753$  and  $\phi \leq 5 \cdot 10^{-2}$ . Equation 7-4 is shown in Figure 7-1 and it is suggested that Equation 7-4 is applicable also for deformation zones. As the hydraulic conductivity may be written as:

$$K = T / B \quad (7-5)$$

where  $B$  [ $L^2T^{-1}$ ;  $m^2/s$ ] is the transmissivity and  $B$  [ $L$ ;  $m$ ] is the geological, Equation 7-4 may be written as:

$$\phi(T) = a \left(\frac{T}{B}\right)^b \quad (7-6)$$

Equation 7-5 implies that the transmissivity increases with the geological width for a constant value of the hydraulic conductivity. How the transmissivity increases with the geological width is generally difficult to determine. The schematic cartoons shown in Figure 7-2 and Figure 7-3 illustrate some common problems.

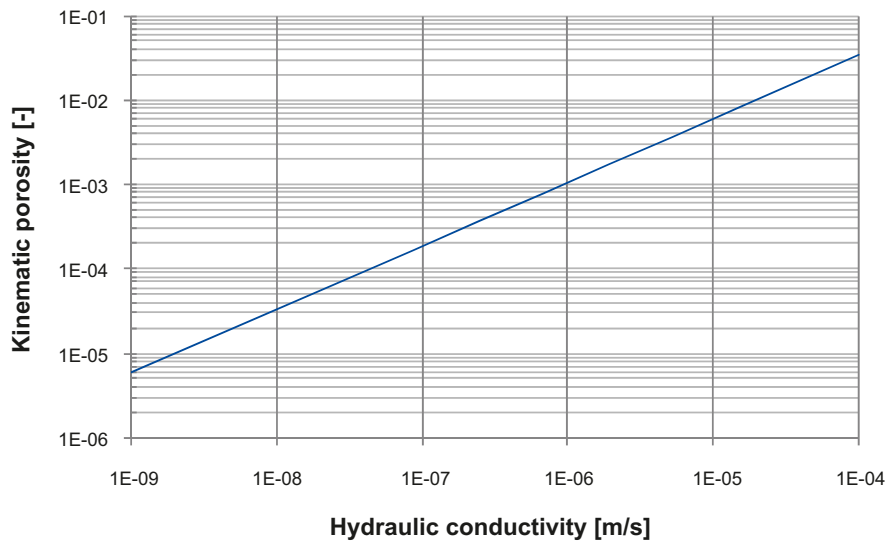


Figure 7-1. Visualisation of Equation 7-4.

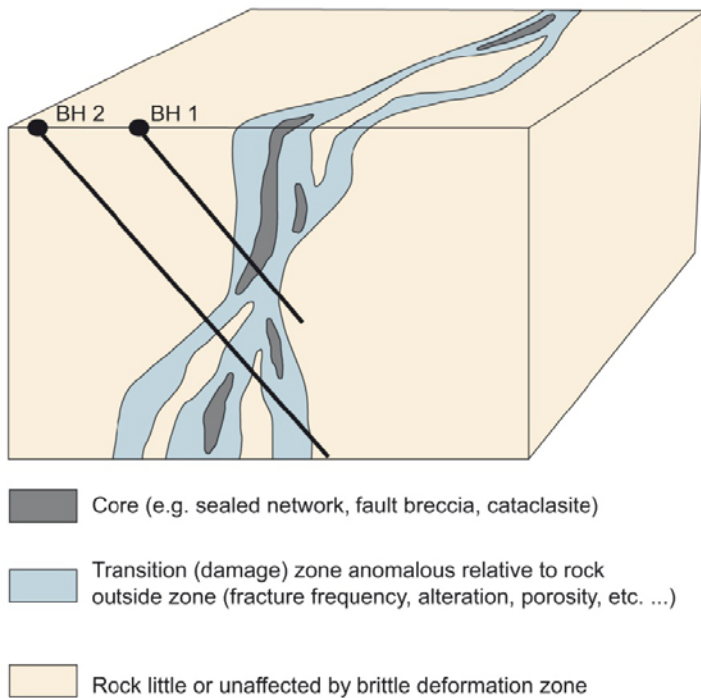
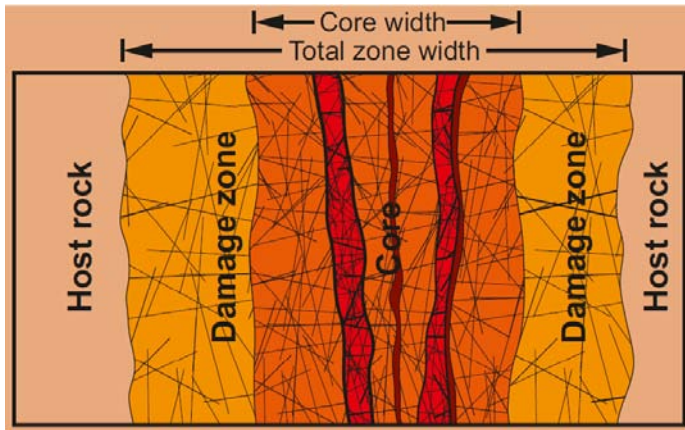


Figure 7-2. Schematic cartoon illustrating the problem to determine the geological width of a deformation zone. Flowing fractures may occur at various places.



**Figure 7-3.** The geological width of a deformation zone may be defined in different ways. In addition, the occurrence and magnitude of transmissive fractures associated with a deformation zone generally varies between different parts of the zone. Some zones are more conductive in the core, others more conductive at the rim between host rock and the damage zone.

Data acquired at Forsmark suggest that the geological width of a deformation zone is approximately 6% of its trace length. Based on this information, the following power-law relationship between geological width and deformation zone transmissivity is suggested here:

$$B = c T^d \tag{7-7}$$

where  $c = 1,000$  and  $d = 0.5$ . Equation 7-7 is shown in Figure 7-4.

Inserting Equation 7-7 into Equation 7-6 gives:

$$\phi(T) = e T^f \tag{7-8}$$

where  $e = a/c^b = 0.19$  and  $f = b(1 - d) = 0.38$ . Equation 7-8 is shown in Figure 7-5.

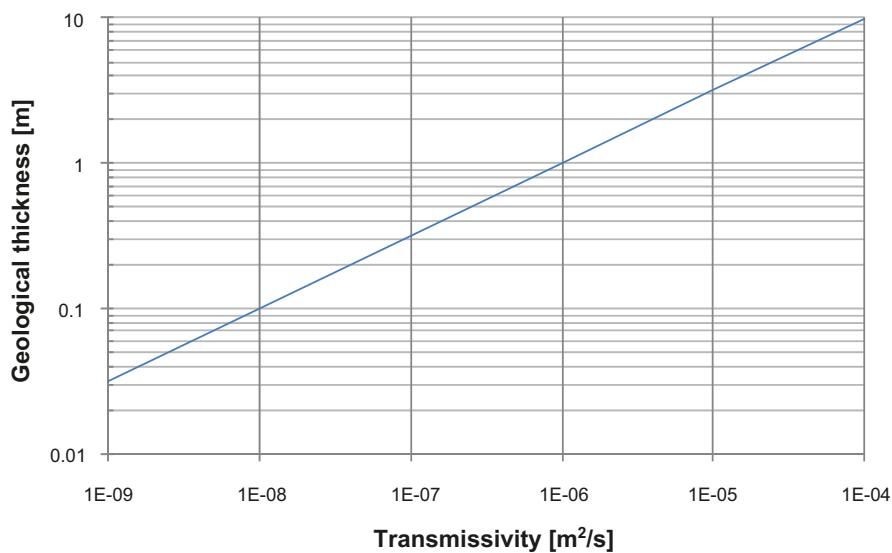


**Figure 7-4.** Visualisation of Equation 7-7.

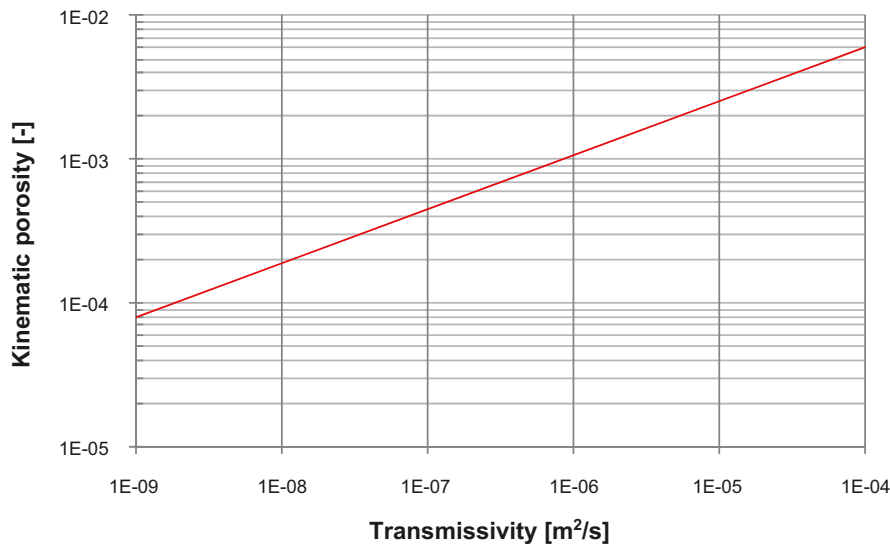


Figure 7-5. Visualisation of Equation 7-8.

### 7.3 Transport aperture

It is noted that the product of the deformation zone kinematic porosity (Equation 7-8) and geological width (Equation 7-7) may be conceived as some kind of deformation zone aperture  $e_B$  [L; m]:

$$e_B = g T^h \quad (7-9)$$

where  $g = a/c^{(1-b)} = 192$  and  $h = b + d - bd = 0.88$ .

/Hjerne et al. 2010/ present a compilation of different types of apertures based on tracer tests performed by SKB. The relationship between fracture transport aperture and fracture transmissivity suggested by /Hjerne et al. 2010/ is:

$$e_t = a T^b \quad (7-10)$$

where  $a = 0.28$  and  $b = 0.3$ . The concept of hydraulic aperture  $e_h$  [L; m] is frequently used in the literature, e.g. in conjunction with the cubic law, which has  $a = 0.01$  and  $b = 1/3$ . Equations 7-9 and 7-10 are shown in Figure 7-6 together with the cubic law.

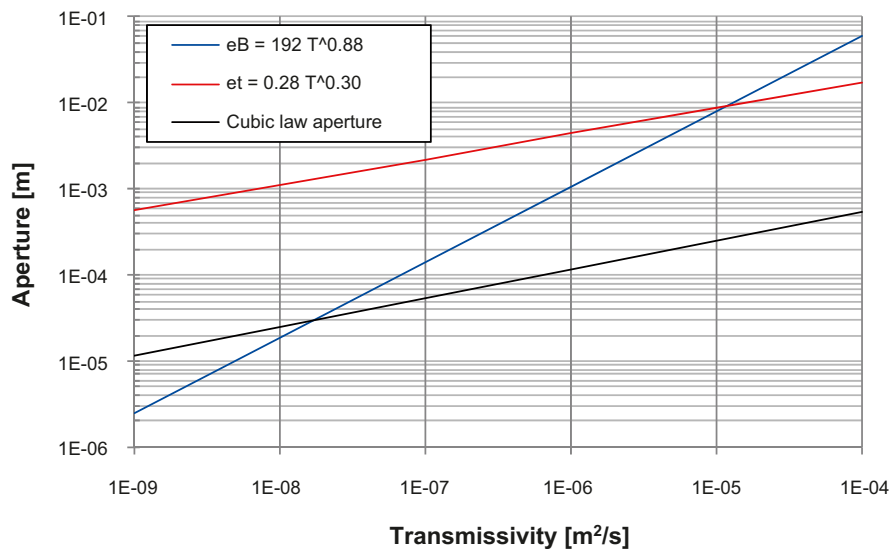


Figure 7-6. Visualisation of Equation 7-10 (red), the Cubic law (black) and Equation 7-9 (blue).

Finally, it is noted that the kinematic porosity of a computational grid cell in an ECPM model may be computed from the total volume of open voids that the underpinning DFN realisation of connected of open fractures creates per unit volume:

$$\phi = \frac{\sum_f e_f a_f}{V} \quad (7-11)$$

where  $a_f$  [ $L^2$ ;  $m^2$ ] is the area of each fracture in the volume  $V$  [ $L^3$ ;  $m^3$ ]. If a truncated DFN realisation is used it is necessary to compensate for the truncation.

## 7.4 Travel time

In a saturated discrete medium, the advective travel time  $t_w$  [T; s] is computed as:

$$t_w = \sum_l \frac{e_l w_f \delta l}{Q_f} \quad (7-12)$$

where  $e_l$  [L; m] is the transport aperture between a pair of fracture intersections,  $\delta l$  is a step length [L; m] along a path of  $l$  steps, each between a pair of fracture intersections,  $w_f$  [L; m] the flow width between the pair of fracture intersections and  $Q_f$  is the flow rate [ $L^3 T^{-1}$ ;  $m^3/s$ ] in the fracture between the pair of fracture intersections.

In a saturated porous medium, the advective travel time  $t_w$  [T; s] is computed as:

$$t_w = \sum_l \frac{\phi \delta l}{q} \quad (7-13)$$

where  $\phi$  [-] is the kinematic (flow) porosity of the saturated porous medium,  $\delta l$  is a step length [L; m] along a path of  $l$  steps and  $q_f$  is the Darcy flux [ $LT^{-1}$ ; m/s].

## 8 Recommendations for flow modellers

### 8.1 General

It is noted that few of the hydraulic investigations at Forsmark, Laxemar and Olkiluoto are deeper than 1 km. Hence, there are great uncertainties involved when hydraulic data from these three sites are adapted to the 5 km deep deformation zone model at the GAP site. In particular, this alert concerns the usage of data from Olkiluoto as there is no depth trend specified at this site.

### 8.2 Usage of HCD properties

Geomodel version 1 does not contain gently dipping deformation zones (Figure 2-5). Gently dipping deformation zones are not modelled at Laxemar either (Figure 8-1). In comparison, both Forsmark and Olkiluoto possess a large number of gently dipping deformation zones.

The structural similarity between Geomodel version 1 and the deformation zone model at Laxemar suggest that hydraulic properties of the steeply dipping deformation zones at Laxemar should be used as the primary hydraulic data set. The transmissivities of the deformation zones at Laxemar show both depth dependence and lateral heterogeneity.

Second, the hydraulic properties of the gently dipping hydro-zones at Olkiluoto should be tried, i.e., despite the difference in dip between the two deformation zone models. The transmissivities of the gently dipping hydro zones at Olkiluoto are fairly high, show weak dependency, and huge lateral heterogeneity.

Third, the hydraulic properties of the steeply dipping deformation zones at Forsmark should be tried. In comparison, the transmissivities of the deformation zones at Forsmark show stronger depth dependence but less lateral heterogeneity compared to the Laxemar data set.

The suggested correlation between the deformation zone sets of Geomodel version 1 and the deformation zone sets modelled at the three Fennoscandian sites is shown in Table 8-1. It is noted that large-scale, gently dipping to horizontal deformation zones are not modelled in Geomodel version 1. This issue needs to be discussed further.

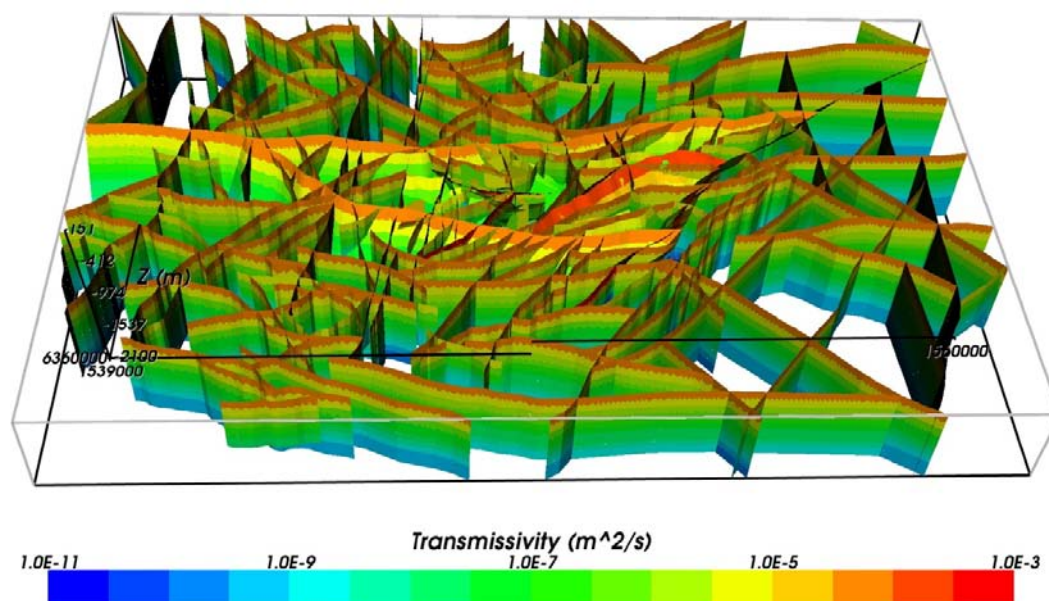


**Figure 8-1.** All HCDs at Laxemar and their inferred depth dependent transmissivity for the deterministic base case model. Oblique view looking from the south.

**Table 8-1. Suggested correlation between the deformation zone sets of Geomodel version 1 and the deformation zone sets modelled at the three Fennoscandian sites.**

Geomodel version 1	Area/Set	Geomodel version 1	Area/Set	Geomodel version 1	Area/Set	Geomodel version 1	Area/Set
ENE-WSW (Lilac)	Laxemar/EW		Laxemar/NW		Laxemar/NE		Laxemar/NS
	Olkiluoto/HZ	NW-SE (Green)	Olkiluoto/HZ	NE-SW (Blue)	Olkiluoto/HZ	NNE-SSW (Black)	Olkiluoto/HZ
	Forsmark/WNW		Forsmark/NW		Forsmark/NE		Forsmark/NNE

### 8.3 Usage of HRD properties

To be consistent with the recommendations made in Section 8.2, HRD data should be used in accordance with the HCD data studied.

Preferably, the ECPM modelling approach should be applied for up-scaling. In the case of CPM modelling, the values of average  $\log(K)$  values as points for regression with depth should be tried. This allows the user to match a continuous function from which grid properties may be derived. In the case of SC modelling, the different standard deviations of  $\log(K)$  should be used as normal random deviates and added to the average  $\log(K)$  values. Autocorrelation may be excluded or included as indicated in the tables provided for each site.

### 8.4 HCD and HRD properties below -1,000 m elevation

It is recommended to start with a model where the hydraulic properties at -1,000 m are retained at all depths below this elevation, i.e., no further depth trend. Second, the approach shown in Figure 8-2 should be applied.

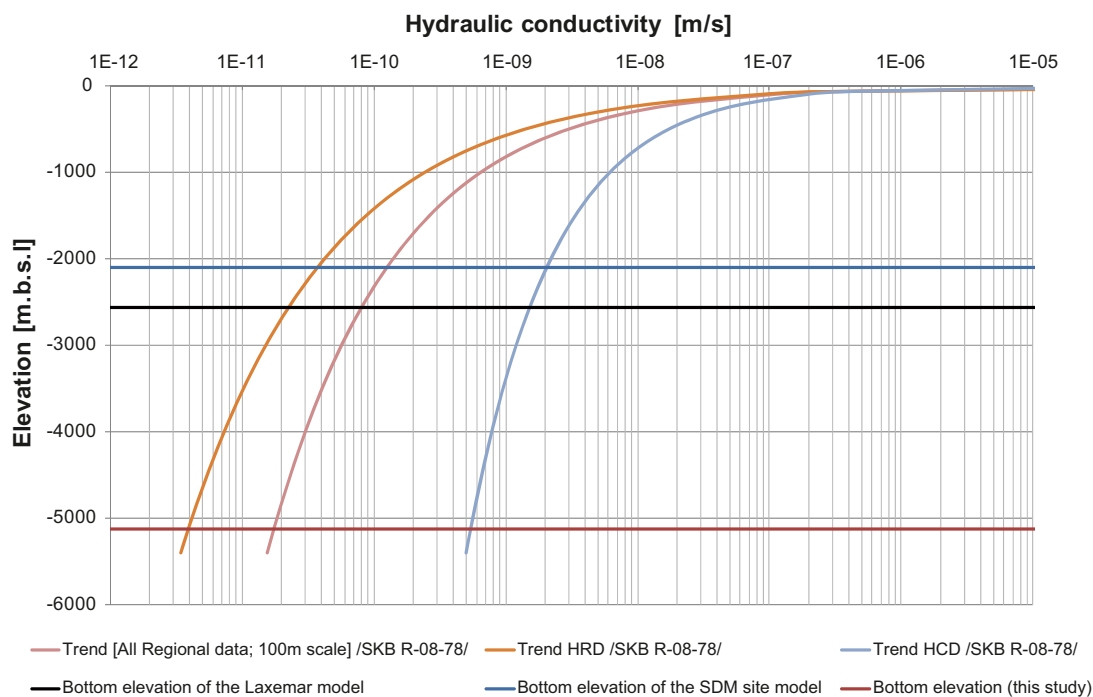


**Figure 8-2.** Illustration of the assessed depth trends at Laxemar /Vidstrand and Rhén 2011/. Note that in this figure the depth trend is not exponential but power-law.



## **8.5 On the modelling of deformation zones outside the area covered by the GAP Geomodel version 1**

For the region outside the area covered by Geomodel version 1, it is suggested to use a deterministic approach, e.g. the approach shown in Figure 8-3. In this figure, Geomodel version 1 is copied and pasted twice to support the extent of the red model domain, cf. Figure 2-7. Inside the area covered by Geomodel version 1, e.g. inside the two yellow model domains, it is suggested that stochastic deformation zones are generated using the DFN properties provided for each site.

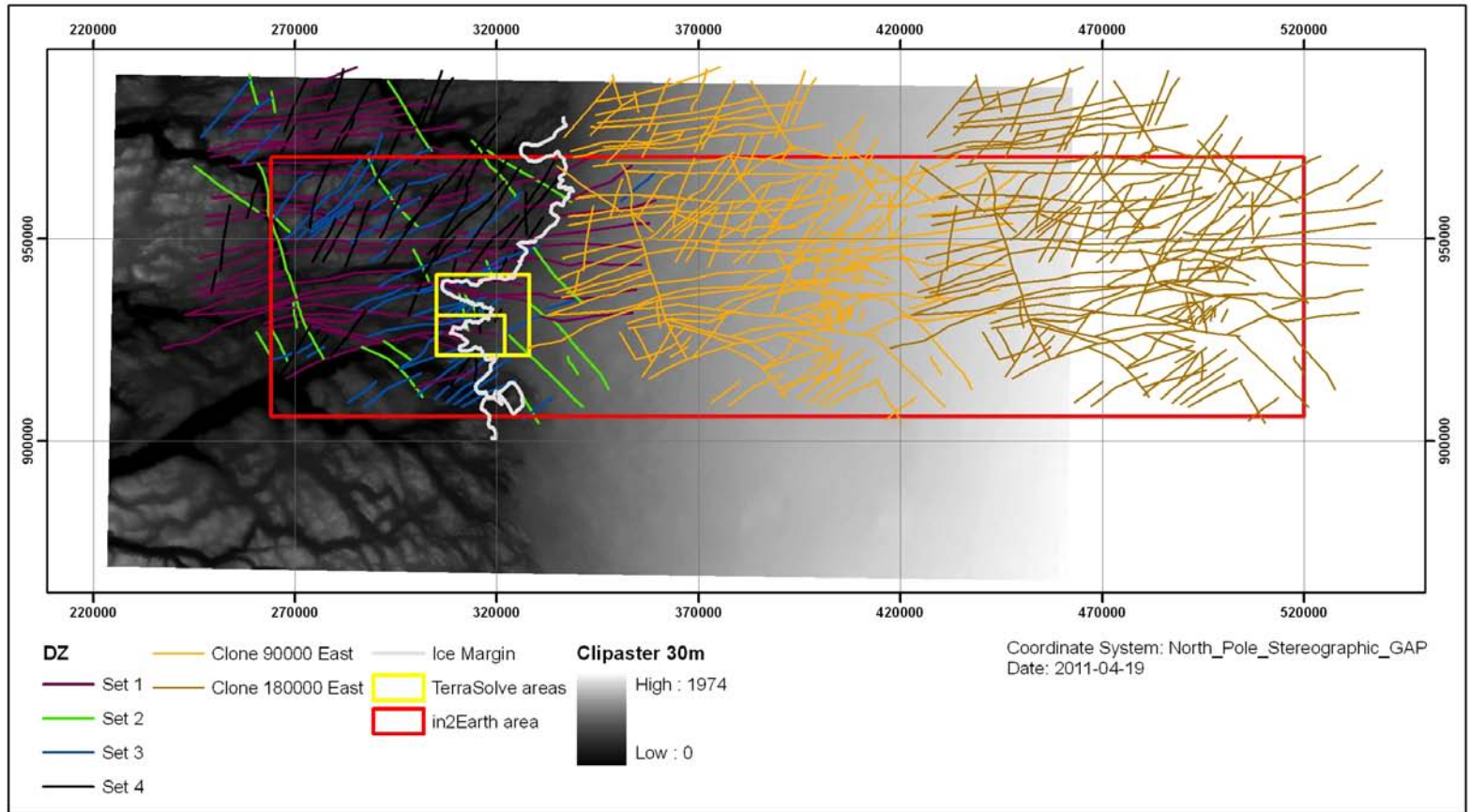


**Figure 8-3.** For the region outside the area covered by Geomodel version 1, it is suggested to use a deterministic approach. That is, Geomodel version 1 is copied and pasted twice to support the extent of the red model domain. Inside the area covered by Geomodel version 1, e.g. inside the two yellow model domains, it is suggested that stochastic deformation zones are generated using the DFN properties provided for each site.

## 9 References

SKB's (Svensk Kärnbränslehantering AB) publications can be found at [www.skb.se/publications](http://www.skb.se/publications).

- Ahokas H, Vaittinen T, Tammisto E, Nummela J, 2007.** Modelling of hydro-zones for layout planning and numerical flow model in 2006. Posiva Working Report 2007-01, Posiva Oy, Finland.
- Bamber J L, Layberry R L, Gogineni S P, 2001.** A new ice thickness and bed data set for the Greenland ice sheet. 1: Measurement, data reduction, and errors. *Journal of Geophysical Research*, 106, pp 33773–33780.
- Engström J, Klint K E, Paananen M, 2011.** The Greenland Analogue Project – Geomodel version 1 of the Kangerlussuaq area on Western Greenland. SKB P-11-38, Svensk Kärnbränslehantering AB.
- Escher A, 1971.** Geologisk kort over Grønland 1:500000, Kort nr. 3: Søndre Strømfjord – Nûgssuaq. De Nationale Geologiske Undersøgelser for Danmark og Grønland.
- Follin S, 2008.** Bedrock hydrogeology Forsmark. Site descriptive modelling, SDM-Site Forsmark. SKB R-08-95, Svensk Kärnbränslehantering AB.
- Follin S, Levén J, Hartley L, Jackson P, Joyce S, Roberts D, Swift B, 2007.** Hydrogeological characterisation and modelling of deformation zones and fracture domains, Forsmark modelling stage 2.2. SKB R-07-48, Svensk Kärnbränslehantering AB.
- Hartley L, Hoek J, Swan D, Roberts D, Joyce S, Follin S, 2009.** Development of a hydrogeological discrete fracture network model for the Olkiluoto site descriptive model 2008. Posiva Working Report 2009-61, Posiva Oy, Finland.
- Hjerne C, Nordqvist R, Harrström J, 2010.** Compilation and analyses of results from cross-hole tracer tests with conservative tracers. SKB R-09-28, Svensk Kärnbränslehantering AB.
- Layberry R L, Bamber J L, 2001.** A new ice thickness and bed data set for the Greenland ice sheet. 2: Relationship between dynamics and basal topography. *Journal of Geophysical Research*, 106, pp 33781–33788.
- Lemieux J-M, Sudicky E A, Peltier W R, Tarasov L, 2008.** Simulating the impact of glaciations on continental groundwater flow systems: 1. Relevant processes and model formulation. *Journal of Geophysical Research*, 113, F03017.
- Rhén I, Forsmark T, Hartley L, Jackson P, Roberts D, Swan D, Gylling B, 2008.** Hydrogeological conceptualisation and parameterisation. Site descriptive modelling, SDM-Site Laxemar. SKB R-08-78, Svensk Kärnbränslehantering AB.
- Rhén I, Hartley L, 2009.** Bedrock hydrogeology Laxemar. Site descriptive modelling, SDM-Site Laxemar. SKB R-08-91, Svensk Kärnbränslehantering AB.
- Vaittinen T, Ahokas H, Nummela J, 2009.** Hydrogeological structure model of the Olkiluoto Site – update in 2008. Posiva Working Report 2009-15, Posiva Oy, Finland.
- Vidstrand P, Rhén I, 2011.** On the role of model depth and hydraulic properties for groundwater flow modelling during glacial climate conditions. SKB R-10-74, Svensk Kärnbränslehantering AB.

### 3D structural-hydraulic model

This appendix describes briefly how a 3D structural-hydraulic deformation zone model has been developed from the GAP Geomodel version 1 together with an explanation of how to use the program package to generate other hydraulic properties of the zones compared to those delivered.

#### A1.1 Development

The basis for the 3D structural-hydraulic model is the shape file describing the 158 lineaments together with the image file containing information of topography. All GIS work is done using ESRI ArcMap 9.3.1.

##### A1.1.1 Indata

The GAP project provided the file “GAP\_Geomodel\_ver1.mxd” together with most of the referenced files. The topography file Clipaster, with topography values in 30 by 30 m squares, was delivered separately to be used in conjunction to the geomodel version 1.

##### A1.1.2 Coordinate system

Though data were delivered using different coordinate systems all data were transformed to the so called BAMBER coordinate system. This coordinate system is based on the Greenland 5km DEM, ice thickness and bedrock elevation grids by /Bamber et al. 2001/ and /Layberry and Bamber 2001/. Data and metadata for this DEM can be located at <http://nsidc.org/data/nsidc-0092.html>. An artefact of the transformation is that the length of the lineament changes, approximately some few percents. According to Ulf Brising (personal comment 20110405) this is due to the coordinate systems being conform, i.e. the coordinate systems keep the angles correct while the lengths can deviate. This cause a mismatch between the lengths recorded in the attribute table coupled to each lineament and the lengths that appear if the coordinates from the shapes are used for calculation.

##### A1.1.3 Export of ESRI GIS data

The geometries of the lineaments was exported to a ESRI shape file which was imported to Surfer 8 (Golden software) using “Base Map” and then exported to an ascii format called bln. The attributes, i.e. “OBJECTID”, “Shape”, “Type”, ”Numbers”, “Description”, “Location”, “SHAPE Length”, “Source”, “Dip” and “Orientation”, was exported to a separate database that was opened by Excel and saved as a csv file. The image file containing the topography was exported to ascii format using the, in ArcMap, built in “raster to ascii” export tool.

##### A1.1.4 Extruding lineaments

A Visual Basic.Net 2010 program called “GAP\_201103\_Creation\_of\_DZ\_model.exe” was written that reads the bln file containing the lineament traces, the file containing the attributes together with the file containing information about the topography. The program first calculates the average orientation of the zone, thereafter adds the z coordinate to the trace, i.e. making it meander in all three directions and to the last extrude the zone perpendicular to the average orientation along the defined dip while triangulating the surface. The zones are extruded between 1,000 m and –5,000 m and the sides of the triangles were rounded to about 1,000 m. If other resolution is needed the program can be run using the instructions in section 0.

##### A1.1.5 Making properties file

A Visual Basic.Net 2010 program called “GAP\_201103\_make\_properties.exe” was written that reads the transmissivity, thickness, storativity, aperture and porosity model for each of the four deformation zone sets together with the zone names and prepare a data file to the DarcyTools input editor described below.

### **A1.1.6 Adding properties**

A Visual Basic 6.0 program called “DT\_input\_Editor\_1.3a.exe” was used to add properties to each triangulated element of each deformation zone. The program was also used to twice clone the deformation zones and paste it 90 km at a time to the east. The program reads the file containing the triangle elements created by “GAP\_201103\_Creation\_of\_DZ\_model.exe” and add the properties in the file created by “GAP\_201103\_make\_properties.exe” the program can also rotate and translate the elements an arbitrary angel and distance.

### **A1.1.7 Making files to be read by DarcyTools**

A FORTRAN code called fractoolsGAP.exe was written to convert the ascii file containing the Deformation zone triangles to the binary DarcyTools V3.1 format. The program reads the file created by “DT\_input\_Editor\_1.3a.exe” and produce a file that can be read by DarcyTools V3.1, or higher, together with a file that can be read by Tecplot.

## **A1.2 Usage of program package**

A brief description of how to run the program package follows below.

### **A1.2.1 Extruding lineaments to deformation zones**

The VB 2010 .Net program GAP\_201103\_Creation\_of\_DZ\_model.exe is used to extrude the 2D lineaments to 3D deformation zones. The program is a console application and needs a data file called indata.txt to be present in the same directory as the program itself. The structure of the file is that each data line is preceded by a heading line describing the data to come. First is the path to the file containing the lineaments defined, thereafter the path to the file containing the GIS properties followed by the path to the file containing the elevation values and to the last the path for the output file. The last three data is regarding the size of the triangles and the top and bottom elevations of the extrusion.

Below is shown the file used to create the delivered files for DarcyTools.

```
traceFileName
DZ_vertices_in_Bamber.bln
orientFileName
dip_and_orientation.txt
zDataFileName
clipaster_in_bamber.txt
OutFileName
triangulated_zones.dti
triangleSize
1000
top coordinate
1000
Bottom coordinate
-5000
```

After the data file is written and saved in the same directory as the program just double click GAP\_201103\_Creation\_of\_DZ\_model.exe or start the command prompt and run the program.

Observe that the program assumes that the order of the zones is the same in both the lineament file and the GIS property file.

### A1.2.2 Create a DZ properties file

The VB 2010 .Net program GAP\_201103\_make\_properties.exe is used to make a property data file that can be read by the DT\_input\_Editor program. The program is a console application and needs a data file called MkePropFileIndata.txt, containing three file paths, to be present in the same directory as the program itself. The structure of the file is that each path is preceded by a heading line describing which file that will be read. First is the path to the file containing the deformation zone properties defined, thereafter the path to the file containing the names of the deformation zones and to the last the path of the output file. Below is shown the file used to create the Laxemar properties.

```
Name of file containing the properties
PropLaxemar.txt
Name of file containing the names of the deformation zones
zoneNames.txt
Output file name
GAP_DZ_Lx_Prop.dat
```

The deformation zone set properties file is constructed using the same approach as the file containing the paths, i.e. pairs of a heading followed by the actual value. The number of deformation zone sets is first defined followed by the DZ set number, transmissivity model, width model, storativity model, and transport aperture model for each set defined. The available models are listed below.

#### Transmissivity model

$$T_{\min} \leq \exp(\log(T_0 \cdot \exp(df \cdot D)) + N[0,1] \cdot sdl \cdot (1 - D/D_{\max})) \leq T_{\max}$$

where

$T_0$  = Transmissivity at zero depth.

$df$  = Decrease factor, how fast the transmissivity is decreasing.

$D$  = Depth, i.e. negative  $Z$  coordinate.

$N[0,1]$  = Normal distribution with zero mean and unit standard deviation.

$sdl$  = Factor to scale the unit standard deviations at zero depth.

$D_{\max}$  = Factor to reduce the deviation at depth, i.e. at depth  $D_{\max}$  the std dev becomes zero.

$T_{\min}$  = Minimum allowed transmissivity.

$T_{\max}$  = Maximum allowed transmissivity.

#### Width model

$B$

where

$B$  = The constant width of the Deformation zone.

#### Storativity model

$$a \cdot T^b$$

where

$a$  = Prefactor

$b$  = Exponent

$T$  = Transmissivity at the actual point.

## Transport aperture model

$$a \cdot T^b$$

where

$a$  = Prefactor

$b$  = Exponent

$T$  = Transmissivity at the actual point.

Observe that data must be separated by semi colon, ";", character.

## Example

An example of the DZ set property file for Laxemar data is shown below.

Number of sets

4

Set name

1

Transmissiv mod (T0; decrFact; NofStdDev; DepthOfZeroSpread; minT; maxT)

8.1E-05; -4.31E-03; 1.35; 5000; 1.00E-09; 2.50E-04

Thickness model (constant value [t=C])

15

Storativity model (prefactor; exponent [S=A\*T^B])

0.00922; 0.785

Aperture model (prefactor; exponent [a=A\*T^B])

0.28; 0.3

Set name

2

Transmissiv mod (T0; decrFact; NofStdDev; DepthOfZeroSpread; minT; maxT)

8.5E-05; -6.31E-03; 1.35; 5000; 1.00E-09; 2.50E-04

Thickness model (constant value [t=C])

15

Storativity model (prefactor; exponent [S=A\*T^B])

0.00922; 0.785

Aperture model (prefactor; exponent [a=A\*T^B])

0.28; 0.3

Set name

3

Transmissiv mod (T0; decrFact; NofStdDev; DepthOfZeroSpread; minT; maxT)

8.5E-05; -6.31E-03; 1.35; 5000; 1.00E-09; 2.50E-04

Thickness model (constant value [t=C])

15

Storativity model (prefactor; exponent [S=A\*T^B])

0.00922; 0.785

Aperture model (prefactor; exponent [a=A\*T^B])

0.28; 0.3

Set name

4

Transmissiv mod (T0; decrFact; NofStdDev; DepthOfZeroSpread; minT; maxT)

8.5E-05; -6.31E-03; 1.35; 5000; 1.00E-09; 2.50E-04

Thickness model (constant value [t=C])

15

Storativity model (prefactor; exponent [S=A\*T^B])

0.00922; 0.785

Aperture model (prefactor; exponent [a=A\*T^B])

0.28; 0.3

After the data files are written just double click GAP\_201103\_make\_properties.exe or start the command prompt and run the program.

The output file contains the properties defined for each of the 158 zones and can be edited manually if any value of a single zone is to be changed. Note, however, that there is no guidance in this file but the data comes in the same order as in the deformation zone set properties file.

### A1.2.3 Adding properties to deformation zones

The Visual Basic 6.0 program DT\_input\_Editor\_1.3a.exe is a windows application where data are fed into different boxes rather than writing an input file. The main window is shown in Figure A-1.

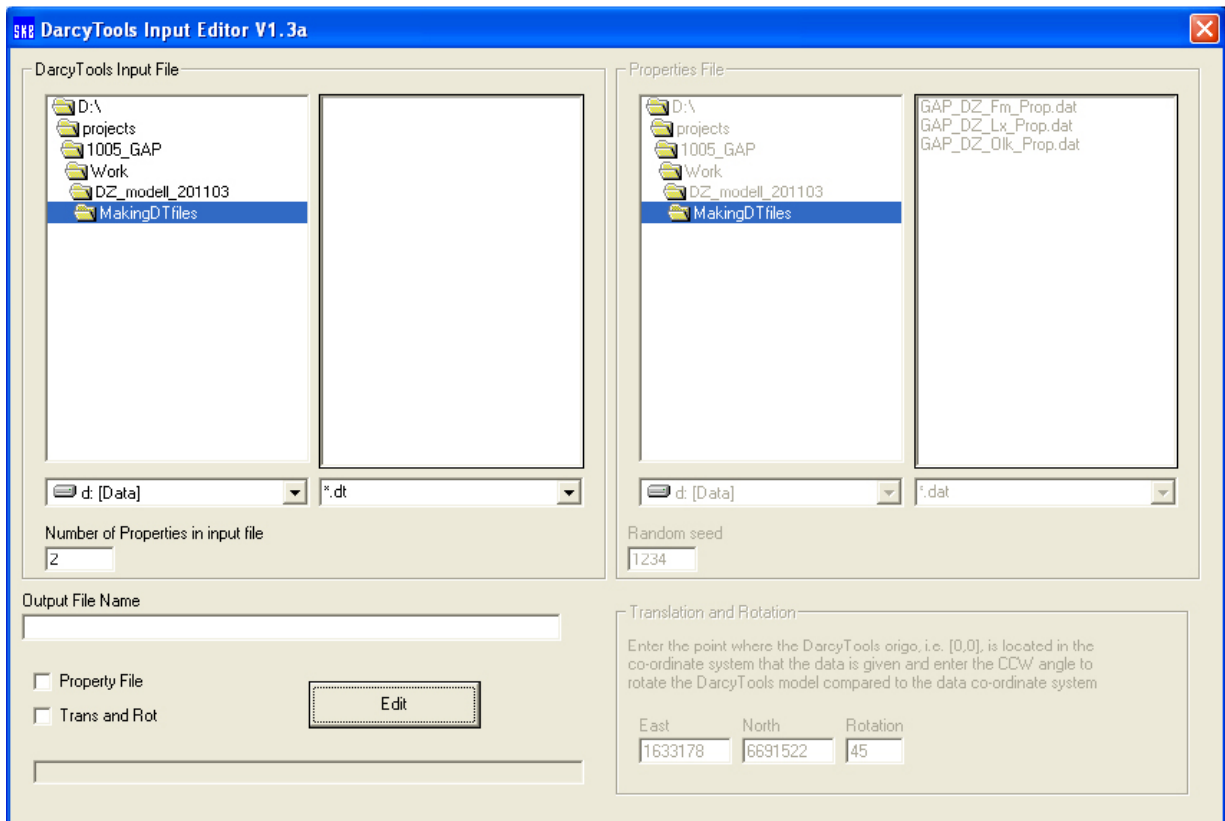


**Figure A-1.** The main window of DarcyTools Input Editor.



To add properties to the geometry file carry out the following 7 steps:

- 1) Browse and mark the file containing the triangulated deformation zones in the Darcy Tools Input File frame (you have to change the filter to \*.dti or \*.\*).
- 2) Change the number of properties to 4 in the Darcy Tools Input File frame.
- 3) Edit the output file name to a suitable name.
- 4) Check the checkbox ahead of the text Property File.
- 5) Browse and mark the file containing the properties for each DZ in the Properties File frame.
- 6) Change the seed to a preferential number.
- 7) Hit the Edit button and wait for the progress bar to show that the program has finished.

#### **A1.2.4 Clone Deformation zones**

The Visual Basic 6.0 program DT\_input\_Editor\_1.3a.exe is a windows application where data are fed into different boxes rather than writing an input file. The main window is shown in Figure A-1

To make a translated copy of the DZ model (with or without properties) carry out the following 6 steps:

1. Browse and mark the file containing the deformation zones in the Darcy Tools Input File frame (you have to change the filter to \*.dti or \*.\*).
2. Change the number of properties to 4 in the Darcy Tools Input File frame.
3. Edit the output file name to a suitable name.
4. Check the checkbox ahead of the text Trans and Rot.
5. Enter the desired amount of translation in the Translation and Rotation frame.
6. Hit the Edit button and wait for the progress bar to show that the program has finished.

#### **A1.2.5 Convert to DarcyTools format**

The FORTRAN program fractoolsGAP.exe is used to convert the DZ file to a format that can be read by DarcyTools V3.1 or higher. The program is a console application and needs a data file called dti2dt\_input.txt, containing three file paths, to be present in the same directory as the program itself. The structure of the file is that each path is preceded by a heading line describing which file that will be read. First is the path to the file containing the triangulated deformation zones with properties, thereafter the path to the file that can be read by DarcyTools and to the last the path to a file that can be visualised using Tecplot. Below is shown the file used to create the Laxemar properties.

```
DZ file name
Laxemar_0.dti
DarcyTools file name
Laxemar_0
Tecplot file name
Laxemar_0.dat
```